Proton-Coupled Electron Transfer in Cytochrome Oxidase

Ville R. I. Kaila,† Michael I. Verkhovsky, and Mårten Wikström*

Helsinki Bioenergetics Group, Structural Biology and Biophysics Program, Institute of Biotechnology, University of Helsinki, P.O. Box 65, FI-00014 Helsinki, Finland

Received June 30, 2010

Contents

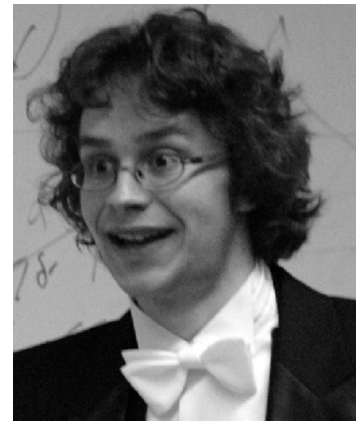

Ville R. I. Kaila was born in 1983 in Helsinki, Finland. He received his M.Sc. in 2006 and his Ph.D. in 2009 in biochemistry from the University of Helsinki, studying the mechanism of proton-coupled electron transfer in cytochrome *c* oxidase in Prof. Mårten Wikström's group. After his Ph.D., Kaila worked as a postdoctoral fellow in the groups of Prof. Dage Sundholm and Prof. Wikström at the University of Helsinki. Currently, he is working as an EMBO long-term research fellow at the Laboratory of Chemical Physics, National Institutes of Health, Bethesda, MA, in Dr. Gerhard Hummer's group, studying the principles of enzymatic proton-coupled electron transfer processes. He has also studied classical violin at the Sibelius Academy, Helsinki, Finland, and actively performs as a musician.

1. Introduction

Enzyme reactions that involve strong coupling between proton and electron transfer are of fundamental importance in biology. This is particularly evident in the reactions of primary biological energy transduction in photosynthesis and respiration, where electron transfer in membranes leads to generation of a trans-membrane electrochemical proton gradient, Peter Mitchell's proton motive force.[1] Here we will focus on the final step of aerobic respiration in which cytochrome *c* oxidase (C*c*O) in mitochondrial and bacterial membranes catalyzes electron and proton transfer to dioxygen, which is reduced to water. The exergonic chemistry catalyzed by C*c*O, which is responsible for the vast majority of O_2 consumed by biological processes,[2] is coupled to endergonic proton translocation across the membrane.[3] The created proton motive force is used secondarily as a driving force for the synthesis of ATP and for other energy-requiring reactions. Thus, understanding the principles of proton-coupled electron transfer is a prerequisite for the understanding of the basic mechanisms of molecular bioenergetics.

C*c*O harnesses the high oxidizing potential of O_2 by utilizing it as a sustained sink for the electrons in the respiratory chain that ultimately derive from the oxidation of hydrocarbon foodstuffs in earlier catabolic reactions.[2] At the same time, the membrane-bound C*c*O functions as a molecular machine that captures free energy from the local redox reaction and transduces it into an easily utilizable delocalized trans-membrane potential form. From a physiological viewpoint, the reactions catalyzed by C*c*O may therefore be more adequately described as electron-coupled proton transfers than as PCET.

The overall reaction catalyzed by C*c*O may be written

$$8H^+(N) + 4e^-(P) + O_2 \rightarrow 2H_2O + 4H^+(P) \quad (1)$$

where N and P denote the negatively and positively charged sides of the membrane, respectively. Equation 1 shows that

* To whom correspondence should be addressed. E-mail: marten.wikstrom@helsinki.fi.
† Current affiliation: Laboratory of Chemical Physics, National Institute of Diabetes and Digestive and Kidney Diseases, National Institutes of Health, Bethesda, Maryland 20892-0520.

10.1021/cr1002003
Published on Web 11/05/2010

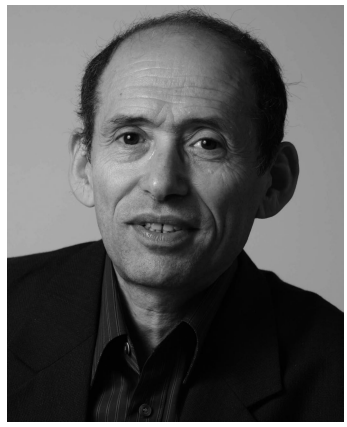

Michael I. Verkhovsky was born in Ukraine, former USSR, in 1953. He received his Master's degree in biophysics at the Lomonosov Moscow State University in 1975 and his Ph.D. in 1981 at the same university, working on the primary mechanisms of bacterial photosynthesis under the direction of Prof. Andrei B. Rubin. From 1989, he worked as a research scientist on bacterial bioenergetics at the Belozersky Laboratory of Molecular Biology and Bioorganic Chemistry, headed by Prof. Vladimir P. Skulachev. In 1991 he was invited by Prof. Mårten Wikström to work on the molecular mechanisms of proton translocation by the respiratory enzymes at the University of Helsinki. Since then these coauthors have had a fruitful collaboration. In the period 1996−2006 he was appointed acting professor at this university, and from 2005 he has been a Group Leader at the Institute of Biotechnology. His research interests are in mechanisms of energy transduction in biological systems, in particular the mechanisms of transformation of redox energy (free energy of electrons) into the energy of ion gradients across biological membranes.

Mårten Wikström received his MD, Ph.D. at the University of Helsinki in 1971, after which he spent a year as a postdoctoral researcher at the University of Amsterdam with Prof. E. C. Slater. In 1975−1976 he was visiting associate professor at the University of Pennsylvania with Prof. Britton Chance. He worked as an assistant professor at the University of Helsinki until 1983, when he was appointed to a personal Chair in medical chemistry (changed to physical biochemistry in 2002). Since 1998 he has been Research Director of the Structural Biology and Biophysics Program of the Institute of Biotechnology. In the period 1996−2006 he was Research Professor of the Academy of Finland. He is a recipient of the Anniversary Prize of the Federation of European Biochemical Societies (FEBS) in 1977, the Scandinavian Anders Jahre Prize in medicine in 1984 and 1996, and the David Keilin Prize and Medal (British Biochemical Society) in 1997, and he gave the Peter Mitchell Medal Lecture in 2000. He was elected a member of Societas Scientiarum Fennica (1982), the European Molecular Biology Organization (1985), The Royal Swedish Academy of Sciences (chemistry, 1992), and Academia Europaea (2010). His research interests are in molecular bioenergetics, membrane proteins, electron transfer, proton translocation, and mitochondrial diseases.

for each electron transferred to O_2 there is translocation of two electrical charges across the membrane.[3] One of these translocated charges results from the "chemistry", i.e. the transfer of an electron from the donor, cytochrome *c*, on the P-side to the active site $\sim^1/_3$ into the membrane (Figure 1), and the transfer of a proton to the same site from the N-side, nullifying the charge of the electron and carrying out part of the O_2 reduction chemistry. The other charge results from the "physics", *viz*. the translocation of another proton (per electron) from the N- to the P-side, coupled to the chemical reaction. The mechanism of this latter proton "pumping" function constitutes one of the major riddles of molecular bioenergetics, and indeed of biochemistry more generally.[4,5]

The overall energetics of the C*c*O reaction is governed by the redox potentials of the electron donor (cytochrome *c*) and the acceptor (O_2). The $E_{m,7}$ for cytochrome *c* is close to 270 mV[6] and independent of pH in the physiological range. The $E_{m,7}$ of the O_2/H_2O redox couple is ~810 mV (Table 1), which refers to a standard state of 1 atm O_2 (~1.23 mM in pure water at 25 °C) and pH 7. At the O_2 concentrations in mammalian tissues (~5−30 μM),[12] the potential would be ~780 mV. Since cytochrome *c* runs less than 30% reduced in typical mitochondrial aerobic steady states, we take its potential to be ~300 mV. Thus, the driving force of the C*c*O reaction is of the order of 0.5 eV per electron, or 2.0 eV (~46 kcal/mol) for the overall proton-coupled four-electron reaction. Table 1 summarizes the thermodynamics of reduction of O_2 to water in aqueous solution. The four one-electron steps involve the reactive oxygen species superoxide ($O_2^{*/-}$), hydrogen peroxide (H_2O_2), and the hydroxyl radical (OH*). It is remarkable that none of these toxic compounds is released in measurable amounts during C*c*O catalysis, despite the fact that the oxygen reduction site receives one electron at a time (see below).

Proton transfer in C*c*O is strongly correlated with electron transfer through the metal sites (Figure 1), in the order Cu_A, heme *a*, and the binuclear oxygen reduction center (BNC) consisting of heme a_3 and the copper ion Cu_B. Heme a_3 is high spin with a proximal histidine ligand (His-376), with the heme iron being magnetically coupled to the Cu_B ion in its immediate vicinity on the distal side. Cu_B is coordinated by three histidines (His-240, His-290, His-291), of which His-240 is post-translationally cross-linked to a tyrosine residue (Tyr-244),[11,13] which modifies both the proton and electron affinities of the tyrosine.[13−15] [If not noted otherwise, the amino acid numbering refers to subunit I of cytochrome *c* oxidase from bovine heart.] Heme *a*, the direct electron donor to the BNC, is a low spin bis-imidazole-ligated heme that lies very close to heme a_3 (edge-to-edge distance ~7 Å; Figure 1). The Cu_A center at the membrane surface consists of two close-lying copper ions, yet functioning as a one-electron redox couple that accepts electrons from cytochrome *c*.

The protons are taken up from the N-side of the membrane (eq 1) by specific proton-conduction pathways, the so-called D- and K-channels, named after Asp-91 and Lys-319, respectively (Figure 1).[16−18] The precise path by which the pumped protons are released on the P-side is not known, but it is likely that the propionate substituents of heme a_3 are involved (see below). The PCET scenario in C*c*O differs from those in many other enzyme systems in which the protons and the electrons are close in space and where quantum mechanical effects are dominant. At the often much longer proton−electron distances in C*c*O, their interactions are instead dominated by classical electrostatics. Another way of looking at this is via the Heisenberg uncertainty principle. At 310 K the positional uncertainty for a proton is ~0.2 Å,

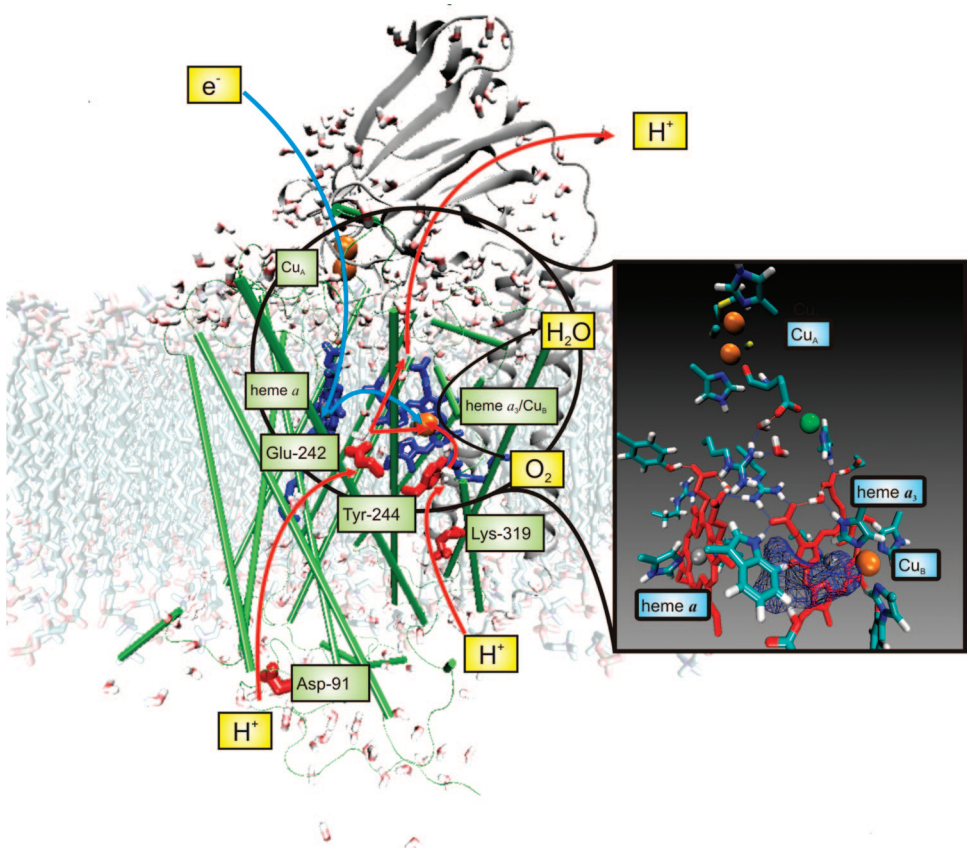

Figure 1. Electron and proton paths in C*c*O based on the X-ray structure of the bovine enzyme.[7] Stepwise electron transfer from cyt *c* (not shown) to Cu_A, heme *a*, and heme a_3/Cu_B (blue lines) couples to proton transfer (red lines). The figure shows some critical amino acids of the D-channel (Asp-91, Glu-242) and the K-channel (Lys-319, Tyr-244). From Glu-242 the proton pathway bifurcates to the proton-loading site (PLS) and the active site of oxygen reduction (BNC; see text). Inset: electron transfer sites of C*c*O and their immediate surroundings. The copper atoms of Cu_A ligate to His- 161, His-204, Cys-196, Cys-200, Met-207, and the backbone of Glu-198. The iron atom of heme *a* coordinates to His-378 and His-61, Arg-38 donates a hydrogen bond to the heme *a* formyl group, and the heme *a* propionates interact with Tyr-54, Trp-126, Arg-438, and Arg-439. The iron of heme a_3 ligates to His-376, and the heme a_3 propionates interact with Trp-126, Arg-439, Asp-364, and His-368. Cu_B coordinates to His-291, His-290, and His-240, which is cross-linked to Tyr-244. The figure also shows Glu-242, the nonpolar cavity above this residue, and the nonredox active Mg/Mn metal site (green sphere). The figure was prepared with VMD.[8]

but it is ~10 Å for an electron, which roughly defines the limits where proton and electron tunneling is significant and how their wave functions are delocalized. A high kinetic isotope effect (KIE) is often taken as an indication for significant proton tunneling.[19] KIE values of 80 or higher are, for example, found in soybean lipo-oxygenase, which catalyzes hydrogen atom abstraction from linoleic acid.[20] In comparison, the KIE's of various partial reactions in C*c*O are only *ca.* 1.5−7.[21,22] On the other hand, as we shall elaborate in this review, electron tunneling via the metal centers creates strong electric fields that direct and control the motion of the protons. These electric fields polarize functionally important water molecules within the protein structure that help to carry the proton from donor to acceptor.

Table 1. Reduction of Dioxygen to Water via Peroxide at pH 7

reaction	$E_{m,7}$[a] (V)
$O_2 + e^- \rightarrow O_2^{\bullet -}$	−0.14 (+0.04[b])
$O_2^{\bullet -} + e^- + 2H^+ \rightarrow H_2O_2$	+0.70
$H_2O_2 + e^- + H^+ \rightarrow HO^\bullet + H_2O$	+0.38
$HO^\bullet + e^- + H^+ \rightarrow H_2O$	+2.31
$^1/_4O_2 + e^- + H^+ \rightarrow {}^1/_2H_2O$	+0.81 (+0.86[b])

[a] Redox potentials versus NHE in an aqueous solution at pH 7. The standard state of O_2 refers to a fugacity of 1 atm, for other species 1*m*. Temperature 25 °C. Data from ref 9 except the $E_{m,7}$ for $O_2/O_2^{\bullet -}$ (ref 10), from which the $E_{m,7}$ of $O_2^{\bullet -}/H_2O_2$ was recalculated. [b] $E_{m,7}$ at a unit activity of O_2.

2. Transfer of Electrons and Protons

2.1. Electron Transfer

The theory of proton-coupled electron transfer has its foundation in the electron transfer (eT) theory developed by Marcus,[23−27] which relates the rate of eT to the free energy change ΔG and the reorganization energy λ. The latter describes the energetics of how much the geometry of the electron donor and acceptor changes upon transfer of the electron. The rate of eT may be written

$$k_{eT} = \frac{2\pi}{\hbar}|H_{AB}|^2 \frac{1}{\sqrt{4\pi\lambda kT}} \exp\left(-\frac{(\Delta G + \lambda)^2}{4\lambda kT}\right) \quad (2)$$

where H_{AB}, the electronic coupling matrix element, is a measure of the strength of interaction between the electron donor and acceptor. The coupling depends exponentially on the distance between donor and acceptor so that[28−30]

$$H_{AB}(r) = H_{AB}(r_0) \exp\left[-\frac{\beta(r - r_0)}{2}\right] \quad (3)$$

The exponential distance dependence of the rate of eT has been confirmed in a wide variety of biological systems.[29,31−33] When quantum effects are included, a vibrational dependence of the reorganization is obtained,[30,34]

$$k_{eT} = \frac{2\pi}{\hbar}|H_{AB}|^2 \left(\frac{\upsilon + 1}{\upsilon}\right)^{P/2} I_\alpha(2S\sqrt{\upsilon(\upsilon + 1)}) \exp(-2S(\upsilon + 1)) \quad (4)$$

where S and P are the reorganization energy and driving force normalized by the average harmonic vibrational frequency (ω), I_α is a modified Bessel function of order α, and $\upsilon = [\exp(-h\omega/2\pi kT) - 1]^{-1}$. Determination of reorganization energies requires evaluation of the average harmonic vibrational frequency of atoms participating in the reactions, the corresponding energy of which is often taken as 60 meV (∼5/2RT) at 310 K. In comparison to the classical Marcus treatment, the quantum-corrected expression has a weaker temperature dependence, which is why determination of the reorganization energy from the temperature dependence of the rate and driving force is difficult (Figure 2).

Moser, Dutton, and co-workers[32,33,35] introduced an empirical expression for the rate of electron tunneling, the so-called Moser−Dutton rule. This expression is based on empirical fitting of extensive eT rate measurements in photosynthetic reaction centers and other electron transfer proteins to the Marcus expression, with a quantum-mechanical correction.[32,33] The rate of an exergonic electron transfer reaction may then be written as

$$\log(k_{eT}) = 13 - (1.2 - 0.8\rho)(R - 3.6) - 3.1\frac{(\Delta G + \lambda)^2}{\lambda} \quad (5)$$

where ρ is the density of protein packing between donor and acceptor.[32,33] The Moser−Dutton theory has been successfully applied to a wide variety of pure electron transfer reactions.

Biological electron transfer rates have also been evaluated by the pathway approach developed by Beratan et al.[36] and based on eT rate measurements reviewed by Winkler and Gray.[37] This approach employs empirical expressions for tunneling rates through covalent bonds, hydrogen bonds, and empty space, which are used to calculate an optimal tunneling pathway for eT (at $\lambda = -\Delta G$) by graph-theoretical means. Treatment of eT by the Moser−Dutton and Beratan−Onuchic approaches yields similar results in most cases and relatively good agreement with experiments. However, there are some interesting cases, such as in cytochrome c oxidase, where agreement between theory and experiments has remained less clear[38−42] (see below).

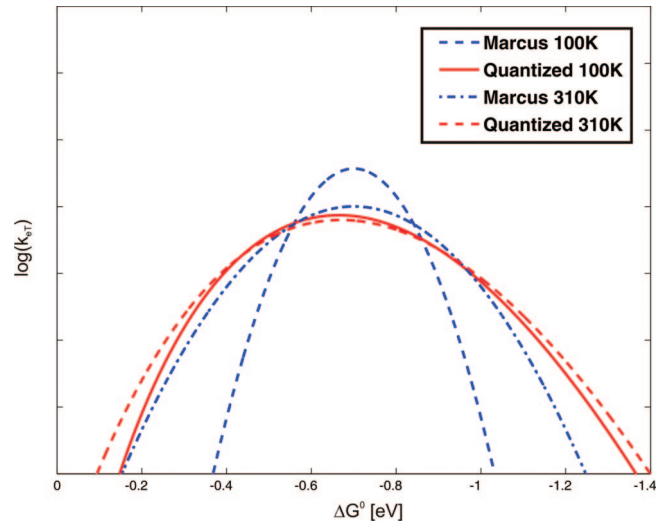

Figure 2. Temperature dependence of the rate of eT predicted by Marcus theory (eq 2) and quantum corrected eT theory (eq 4). The quantum corrected eT theory predicts a much weaker temperature dependence of the eT rate than the semiclassical Marcus theory.

2.2. Proton Transfer

Marcus[24,43] also described proton transfer (pT) and established a relation between the rate of pT, driving force ΔG, $\Delta G_0^{\ddagger}$ (analogous to the reorganization energy), and a "work function" w, representing the work required to bring the reactants together,[44,45]

$$\log(k_{pT}) \propto w + \Delta G_0^{\ddagger}\left(1 + \frac{\Delta G}{4\Delta G_0^{\ddagger}}\right)^2 \quad (6)$$

In contrast to the Brønstedt free-energy relation where $\log(k_{pT})$ depends linearly on the difference in pK_a between the proton donor and acceptor (ΔpK_a), the Marcus pT theory predicts a parabolic dependence. In a narrow ΔpK_a range, this difference may not be visible, but Silverman et al.[44,45] have successfully applied this pT theory on proton transfer reactions of carbonic anhydrase.

Modeling the dynamics of pT reactions requires an accurate description of bond formation and scission, which is not possible in conventional biomolecular force fields. The empirical valence bond (EVB) method, pioneered by Warshel and Weiss[46] and further developed by Schmitt and Voth[47] to the multistate empirical valence bond (MS-EVB) approach, has been applied in studying a wide variety of enzymatic proton transfer reactions, including CcO.[48−53] Other "reactive" force fields in addition to semiempirical and high-level quantum chemical approaches have also been applied to study biological proton transfer reactions,[54−58] albeit to a lesser extent in CcO.

As concluded above, acid dissociation constants (pK_a) are of crucial importance in describing proton-coupled electron transfer reactions. Although extremely challenging, pK_a values within a protein may be approached by continuum electrostatic calculations, which are based on the use of a thermodynamic cycle.[59,60] By estimating the energetics of transferring the deprotonated and protonated forms of an amino acid from bulk water to protein, and using its experimental pK_a in aqueous solution, the pK_a within the protein can be calculated by solving the Poisson−Boltzmann or Generalized-Born equations on a finite grid.[61] The pK_a can be divided into a desolvation part, interaction with

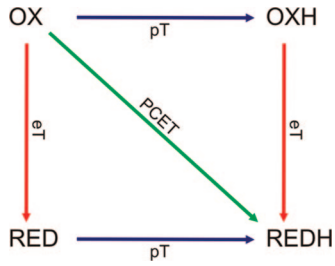

Figure 3. Stepwise and concerted PCET. Abbreviations for electron and proton acceptor sites: OX, oxidized,; OXH, oxidized and protonated; RED, reduced; REDH, reduced and protonated.

background charges within the protein, and the pK_a of the residue in aqueous solution. This yields the intrinsic pK_a (p$K_{a,int}$), which is the pK_a when all other titratable residues in the system are in their neutral form. Monte Carlo sampling[62] may be used to account for the 2^N possible protonation states of a protein with N titratable residues, to get the pK_a at any ionization state. Adding protein dynamics, either from MD simulations[60] or by using a library of typical rotamer conformations,[63,64] increases the accuracy of such calculations considerably. pK_a calculations have been applied to proton-coupled electron transfer reactions in C*c*O by several research groups.[65−74]

Nuclear tunneling effects in proton transfer reactions were incorporated by the pioneering studies of Borgis and Hynes[75,76] and Hwang et al.[77] According to the current view, based on path integral simulations of water,[78] gramicidin,[54,79] and other biological systems,[80] nuclear tunneling is not of significant importance in pure proton transfer reactions.

Proton-coupled electron transfer can be either sequential or concerted[18,81−83] (Figure 3). In the latter special case, the electron and proton transfers are part of the same quantum-chemical event. Hydrogen atom transfer is another special case where the proton and the electron originate in a common donor and are transferred to the same acceptor. In sequential PCET, which is more relevant for C*c*O, either eT or pT occurs first, followed by the other in a separate event. The overall rate will in each case be dependent on which step is rate-limiting. For example, Graige et al.[84] studied the dependence of the rate of reduction of the quinone Q_B on the driving force in a bacterial photosynthetic reaction center, by varying the quinone moiety in the donor Q_A site. In this way they were able to distinguish between the different possible PCET mechanisms outlined in Figure 3. The work by Faller et al.[85] with photosystem II (PSII) demonstrates how the eT and pT components of a PCET reaction may be separated at very low temperatures, at which eT takes place but relaxation due to pT is hindered. As will become evident below, the eT reactions in C*c*O are in most cases either pure tunneling events without coupling to pT or PCET events in which the pT limits the reaction.

Biological proton transfer is usually envisaged to take place by the so-called Grotthuss mechanism,[86−88] which is a kind of bucket brigade mechanism where the proton entering on one side of a transfer chain is not the same as the proton exiting on the other (Figure 4). When pT occurs via water molecules, these are initially polarized toward the proton acceptor; after the pT reaction (the "hop"), the polarity of the water chain is reversed and requires a "turn" for pT to be reinitiated in the same direction. Figure 4 shows snapshots from a short first-principle (DFT) molecular dynamics simulation of proton transfer from a hydronium ion to an imidazole via three water molecules, where the described behavior is observed in agreement with many computational pT studies.[54,78,90−95]

There are some important interrelations between a chain of water molecules, its polarization, and the energetics of proton conduction through that chain by the Grotthuss mechanism that have not been generally appreciated. In electron-coupled proton transfer (e.g., in C*c*O), movement of the electron creates an *electric field* in a domain between the proton donor and acceptor that contributes to the driving force for the proton transfer. Electric fields within microscopic protein structures can be very large when considered on a macroscopic length scale; for example, Lehle et al.[96] measured fields of over 1 V/nm (=10 MV/cm) in a cavity of myoglobin, and our preliminary electrostatic calculations have yielded fields of similar magnitude near the active site of cytochrome oxidase. It is noteworthy that electric fields of this magnitude have been shown to exert substantial effects on water molecules in low polarity environments.[97,98] An electric field of this magnitude provides *attraction for water dipoles* to move into this domain due to the electric field gradient between the domain and its surroundings, an effect related to effects leading to electroporation,[99] and obviously aiding the ensuing pT. Furthermore, *the field orientates the water dipoles* into a chain to aid the proton transfer from donor to acceptor, and *it lowers the barrier of proton transfer* from the donor to the first water molecule in the chain (Figure 5A), which is the step generally thought to limit the overall pT rate. Finally, the existence of an organized chain of several water molecules does itself lower this pT barrier considerably compared to pT to a single water molecule (Figure 5B), in part due to the dipole field of the organized water file and in part due to delocalization of charge in the chain. The electric field near the proton donor is stronger for an aligned and collectively orientated chain of water dipoles, which effectively lowers the barrier for the initial proton transfer from the donor to the chain. The effect of thermodynamic delocalization enhances this electrostatic effect, with the availability of multiple water sites providing an entropic contribution, that lowers the free energy for protonation of the water chain. In addition, quantum-mechanical delocalization in the chain with respect to both electrons and protons might contribute to the lowered barrier.

A concrete example of the above may be seen in the QM/MM simulations of pT in bacteriorhodopsin by Lee and Krauss,[95] where proton transfer from the donor Asp-96 to the acceptor Schiff's base does not take place until the water "wire" connecting them is optimally organized (polarized). This also means (e.g., in MD simulations) that observation of water molecules forming a polarized directional chain from a potential proton donor to an acceptor is indicative of a thermodynamically and kinetically favorable proton transfer route.

Yet another distinction may be made in this connection, *viz*. between "chemical" and "physical" protons, as already briefly alluded to. A "chemical" proton is transferred to the same chemical entity as that receiving the electron, whereas a "physical" proton[81] does not participate in the catalytic chemistry although its movement is coupled to it. Examples of the first category are the protonation of a quinone in photosynthetic reaction centers or PSII,[100] or protonation of oxygen intermediates in formation of the equivalent of water in the active site of C*c*O (see below). The protons pumped across the membrane by C*c*O are an example of the second category. It may be of historical interest to note that Peter

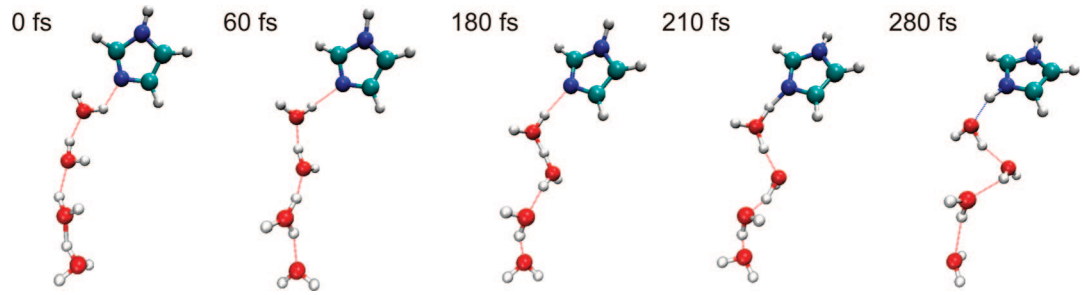

Figure 4. Dynamics of proton transfer from H_3O^+ to imidazole, studied by first-principle molecular dynamics simulations at the BP86/def2-SVP level of theory using TURBOMOLE.[89]

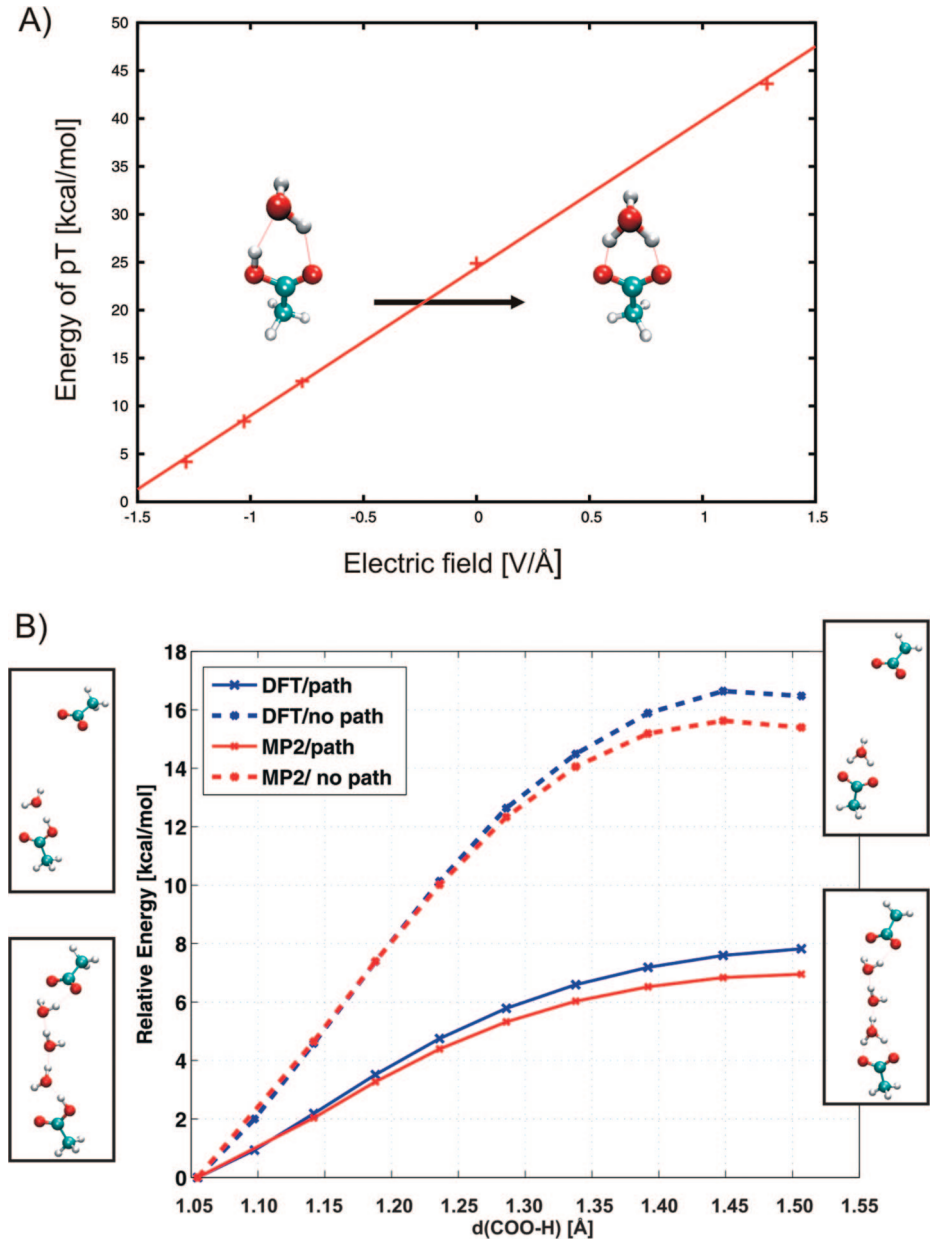

Figure 5. (A) Energy of proton dissociation from a carboxylic acid to a water molecule, as a function of an external electric field at the B3LYP/def2-TZVP level of theory using TURBOMOLE.[89] (B) Energy of proton transfer from a carboxylic group to the nearest neighboring water molecule with and without a water path, studied at the B3LYP/def2-TZVP and MP2/def2-TZVP levels of theory using TURBOMOLE.[89]

Mitchell's chemiosmotic theory[1] was entirely based on "chemical" protons, with the pT and eT components of the PCET reactions being themselves orientated with respect to the two faces of the biological membrane. At the time, such electron−proton coupling was deemed *direct*, as opposed to *indirect* coupling for the case of "physical" protons. Today, it is clear that indirect coupling mechanisms in respiratory and photosynthetic oxidative phosphorylation (as defined here) prevail for the F_1F_0 ATP synthase, for complex I, and for C*c*O.

3. Electron Tunneling in Cytochrome c Oxidase

As it has turned out, the initial electron transfers into C*c*O, from the donor cytochrome *c* to the Cu_A site, and from Cu_A to heme *a*, are not accompanied by proton transfer at the time scale of the eT event itself. The electron transfer between the two heme groups can also be experimentally "isolated" from proton transfer, which has helped us to understand the nature of the eT process but has also created much discussion.

3.1. Reduction of the Primary Electron Transfer Site

Cytochrome *c*, the soluble electron carrier protein in the intermembrane space of mitochondria, shuttles electrons to C*c*O from the cytochrome bc_1 complex of the respiratory chain. Docking of reduced cytochrome *c* is guided by electrostatic forces, via interactions of conserved lysines around the heme crevice of cytochrome *c* and several carboxylate groups in the hydrophilic extramembranous domain of subunit II of C*c*O.[101−104] This domain includes the bimetallic Cu_A center consisting of two copper ions ligated by two histidines, two cysteines, a methionine, and the backbone of a glutamic acid (Figure 1), which serves as the immediate electron acceptor. EPR studies had indicated already before the X-ray structures that oxidized Cu_A is a bimetallic mixed valence center (Cu[1.5]Cu[1.5]),[105] and redox titrations had revealed that oxidoreduction involves a single electron (see references cited in ref 106). Quantum chemical calculations[107] as well as EPR data[108,109] indicate that the two copper ions have identical spin distributions; however, the charge change on oxidoreduction is spread asymmetrically among the copper ligands, which might be of functional importance in electron tunneling. The electrostatic nature of the docking of cytochrome *c* to C*c*O is supported by effects of ionic strength and by mutational experiments. Brownian dynamics simulations predict that protein−protein association can take place at the surprisingly high rate of 2×10^6 M^{-1} s^{-1} without involvement of attractive or steering forces.[110] The second order rate constant for eT from cytochrome *c* to C*c*O[111] is $\sim 2 \times 10^8$ M^{-1} s^{-1}. However, the positively charged cytochrome *c* experiences the negative charge of the membrane surface and does not leave it, thus making delivery of cytochrome *c* to the oxidase a 2D diffusion process. Together with the steering effects, this creates the 2 orders of magnitude enhancement in the rate. The first order rate of eT from heme *c* to Cu_A in the docked complex[111−113] is $\sim 6 \times 10^4$ s^{-1}, which is close to that expected from electron tunneling theory applied on the docked cytochrome *c*−C*c*O structure.[114]

3.2. Reduction of the Secondary Electron Transfer Site

Heme *a* is a six-coordinated low-spin heme that is located approximately $^1/_3$ into the membrane from the P-side (Figure 1). The edge-to-edge distance to heme a_3 in the active site is only ∼7 Å, and this feature is fully conserved within the heme−copper oxidase superfamily of enzymes. Heme *a* accepts electrons from Cu_A and donates electrons—one at a time—to the binuclear site. In shuttling between reduced and oxidized states, the formal charge on the heme iron changes by one unit. However, QM calculations show that this unit change in charge is spread out across the entire porphyrin ring so that the charge change at the iron is only 10−15%.[107,115,116] Such a spread produces a much smaller potential than a localized charge at the same distance and, thus, helps to minimize the energetic cost of eT from Cu_A at the membrane surface to heme *a* within the membrane domain.

The rate of eT from Cu_A to heme *a* varies somewhat depending on the source of enzyme, the methodology, and whether the enzyme is membrane-bound. The measured rates[111,117−123] vary between $2-3 \times 10^4$ s^{-1} and $5-10 \times 10^4$ s^{-1}. Especially the latter rates are in excellent agreement with the rate of 8.7×10^4 s^{-1} predicted from the structure by the Moser−Dutton ruler.[40] In agreement with this, the eT from Cu_A to heme *a* is almost certainly due to pure tunneling because the rate is insensitive to changes in pH and to heavy water substitution.[118,124,125] It seems clear, then, that at least on a fast time scale (<50 μs) the eT from Cu_A to heme *a* is not coupled to the movement of protons. Heme *a* has been named the electron-queuing site[2] because further eT to the binuclear center is strictly controlled by protons, as we shall see.

3.3. Electron Tunneling between the Heme Groups

While the forward eT from heme *a* to the binuclear site is strongly coupled to proton transfer (section 5), there is a method by which pure heme−heme electron tunneling can be measured undisturbed by other events. Initially the binuclear site is trapped in its reduced ferrous/cuprous state and stabilized by carbon monoxide binding to the heme iron, but under conditions where heme *a* and Cu_A are both oxidized. Flash photolysis of the CO from this "mixed valence" form of C*c*O results in ultrafast displacement of CO to bind Cu_B (within a fraction of a picosecond[126]), from where it dissociates with a time constant of ∼3 μs (rebinding of CO occurs later, on a millisecond time scale). It was reported early on that CO dissociation from heme a_3 at neutral or acidic pH led to electron re-equilibration, first by eT to heme *a* ($\tau \sim 3$ μs) and then from both hemes to Cu_A ($\tau \sim 35$ μs[122,123]) and that neither reaction phase was sensitive to pH or heavy water substitution. Consequently, the 3 μs interheme eT was long considered to represent the true tunneling rate, although it is 1000-fold slower than expected on the basis of the Moser−Dutton ruler.[32,33,35] However, measurements of interheme eT in quinol oxidase from *E. coli* indicated the existence of a much faster component.[127] Subsequently, it was proved that the 3 μs event was actually preceded by a much faster phase of eT from heme a_3 to heme *a*,[128] and this reaction was later time-resolved in C*c*O from bovine heart[38] and for heme o_3 to heme *b* in the related quinol oxidase from *E. coli*.[41] In both cases the true electron tunneling rate was reported to be 1/1.4 ns^{-1}, which is precisely the rate predicted by the Moser−Dutton ruler using generic values for λ (0.7 eV) and ρ (0.76) in eq 5, whereas the 3 μs phase was found to be limited by CO dissociation from Cu_B. However, Jasaitis et al.[39] reported λ to be only ∼0.2 eV from measurements of the temperature dependence of the rate and driving force, although the temperature range covered may not have been sufficient[40] (see Figure 2). More recently, Jasaitis et al.[41] speculated that if the reorganization energy is indeed very much lower than the Moser−Dutton generic value, then the very low packing density locally between the heme edges might compensate for an otherwise overestimated eT rate. This work led Beratan and Balabin[42]

to conclude that the heme−heme eT may occur along a unique path between the heme edges. In support of the results by Jasaitis et al.,[39] we have recently found $\lambda \sim 0.2$ eV for the heme−heme eT in independent quantum-chemical and molecular dynamics calculations (Kaila et al., *Proc. Natl. Acad. Sci. USA*, in press). However, we also found that the Moser−Dutton theory predicts the eT rate very well for this low value of λ if the distances (R) between all individual donor and acceptor atoms are paired with their specific values for ρ, and averaging the rates thus obtained from eq 5. In this treatment both the distances (R) and the packing densities (ρ) correspond to the individual feasible donor/acceptor atom pairs, which seems more physically appropriate than combining a single edge-to-edge distance with an average packing density. It is worth pointing out that the results from this version of using eq 5 and the original converge at long donor/acceptor distances. Our finding suggests that there need be no singular specific tunneling path between the two hemes of C*c*O but that all donor and acceptor atoms may contribute to the process.

A further millisecond phase of eT from heme a_3 back to heme a was described to occur after CO photolysis of isolated mixed-valence C*c*O at high pH.[129] This is a PCET reaction in which a proton is released from the BNC from a distal aquo ligand of ferric heme a_3 ($pK_a \sim 9$), specifically via the K-pathway.[129,130] Interestingly, this reaction was reproduced with enzyme incorporated in liposomes,[130] but it then occurred with a much faster rate ($\sim 1/50\ \mu s^{-1}$). It is also of interest to note that the state of the BNC after this electron backflux is Fe[III]−OH^- Cu[I] YOH (where YOH denotes the neutral cross-linked Tyr-244 in the active site), which is the structure proposed independently for the transient E_H intermediate observed in the forward direction of the catalytic cycle after photoinjection of an electron into the oxidized C*c*O.[4]

4. Catalytic Cycle and States of the Binuclear Center

4.1. O_2 Binding and Bond Splitting

Due to its nonpolar properties, the solubility of oxygen in lipid membranes is ~5-fold higher than that in water,[131] which is why one may predict that O_2 diffuses into the active site of C*c*O from the membrane phase. The crystal structures[7,11,132−141] indeed show nonpolar channels that lead from the center of the membrane to the binuclear heme−copper site. Mutational[142] and xenon labeling[135] experiments as well as molecular dynamics simulations[143] all support the view of channels for unimpeded oxygen diffusion, which also explains the very fast interaction of O_2 with the reduced active site[124,144−146] ($\sim 1.4 \times 10^8\ M^{-1}\ s^{-1}$). The resulting heme−oxygen adduct, Compound A,[144] is strongly reminiscent of the corresponding heme structures of oxyhemoglobin or oxymyoglobin (Figure 6). The dissociation constant of Compound A is 0.28 mM, making the off rate[144,146,147] almost 40,000 s^{-1}, which seems curious at first sight, considering the O_2 concentrations in tissues (5−30 μM)[12] and that the Michaelis constant (K_M) for oxygen is in the low micromolar or submicromolar range.[147,148] As first demonstrated by Chance et al.[144] in low-temperature experiments, the high apparent oxygen affinity (which is of obvious physiological importance) is in part due to fast trapping of the oxygen once bound to the active site, relative to a much slower rate of turnover.[147] The high rate of oxygen diffusion to the site via nonpolar "channels" also contributes to the low K_M value.[142]

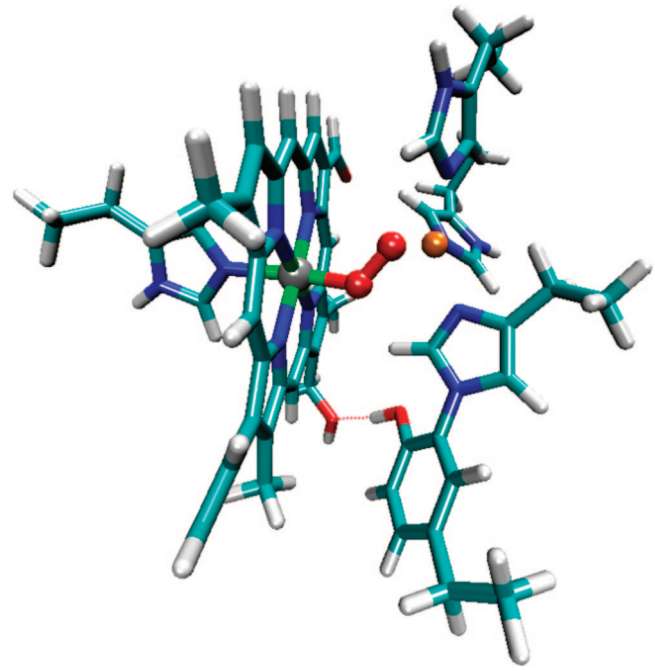

Figure 6. Quantum chemically optimized structure of Cmpd A (at the BP86/def2-SVP(C,H,N,O)/def2-TZVP(Fe,Cu) level of theory) using TURBOMOLE.[89] The O−O bond length increases to 1.32 Å, from the bond length of isolated O_2 of 1.22 Å, due to electron transfer from heme a_3. The observed O−O bond length compares well with the O−O bond length of 1.35 Å obtained for isolated superoxide.

After O_2 binds to the fully reduced C*c*O (in *ca.* 10 μs at 300 K and 1 mM O_2),[124,146] the O−O bond is cleaved in *ca.* 25 μs (somewhat depending on the source of C*c*O). The reaction includes eT from heme a to the binuclear site (BNC), and the latter forms the so-called P_R state. In contrast, if only the BNC is reduced prior to the reaction with O_2, oxygen binding is again followed by bond splitting (now in *ca.* 200 μs) and generation of the so-called P_M state. The P-state nomenclature originates from the early belief that this state is a ferric/cupric/peroxy intermediate. The reason was that this state was formed in intact mitochondria by a two-electron oxidation of the ferric/cupric site by reversal of part of the catalytic cycle at a high proton electrochemical gradient across the mitochondrial membrane and a high redox potential at the acceptor, cytochrome *c*.[149] Weng and Baker[150] were the first to point out that the optical spectrum of P in the Soret region (P_M and P_R have the same optical spectra)[151] is virtually identical to that of the next intermediate, the F state (see below), in which heme a_3 is in the ferryl state, as originally suggested.[149] Hence, it was suggested that O−O bond scission had occurred already in the P states[150] and that heme a_3 has the ferryl structure. Subsequent Raman work, especially by Proshlyakov et al.,[152−154] and an ingenious mass spectrometric oxygen labeling experiment by Fabian et al.[155] proved this to be the case (see also ref 156). While the optical characteristics of P_M and P_R are the same, the latter shows a unique EPR signal from cupric Cu_B,[157] the hyperfine structure of which is broadened by using $^{17}O_2$ in the reaction,[158] indicating a fourth oxygenous copper ligand. The most likely structure of the P_R state is thus a ferryl heme (Fe[IV]=O^{2-}) and Cu[II]−OH^-, where the two oxygen atoms stem from O_2 (Figures 7, 8). The reaction involves transfer of four electrons to dioxygen, two from ferrous heme iron, one from

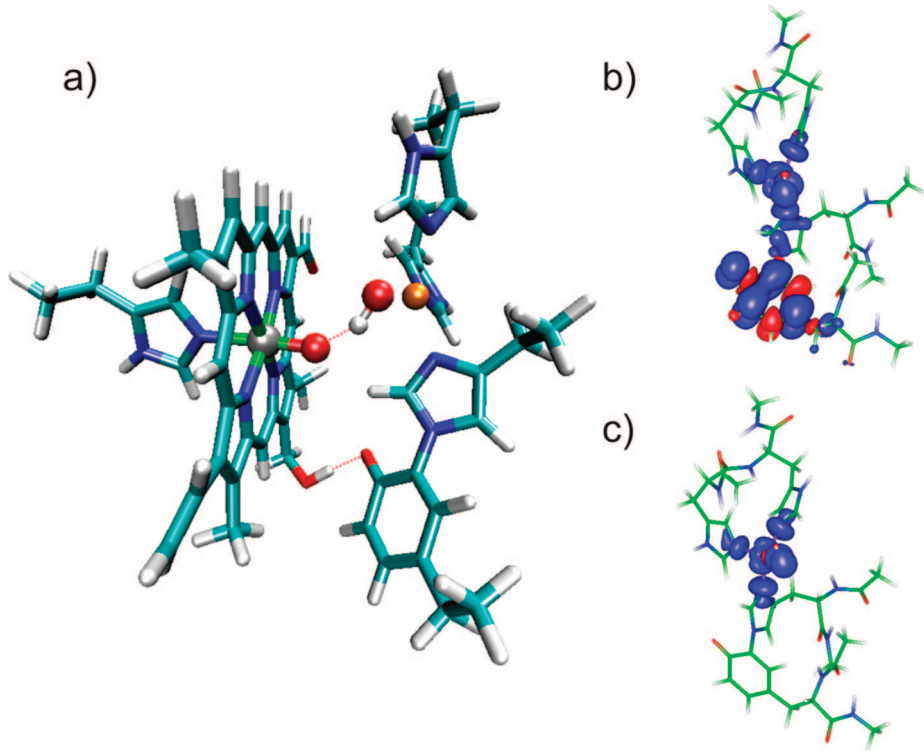

Figure 7. (a) Quantum chemically optimized structure of the P_M state (at BP86/def2-SVP(C,H,N,O)/def2-TZVP(Fe,Cu) level of theory) using TURBOMOLE.[89] The O−O distance between the iron and copper ligands is 2.48 Å, typical for an ordinary hydrogen bond (d(O−H) = 1.59 Å). (b) Spin distribution in the Cu_B center in the P_M and (c) P_R states obtained at the B3LYP/def2-TZVP/ε = 4 level of theory.[14] In the former state, almost a unit spin resides on Tyr-244 in addition to the unpaired electron of Cu[II]. VMD[8] and gOpenMol[159,160] were used for visualization.

cuprous Cu_B, and one from heme *a*. Recent FTIR data suggested that the proton required in O−O bond scission originates from the unique cross-linked tyrosine in the site.[161] The structure of the P_M state is probably the same (Figures 7 and 8), except for the origin of the fourth electron, which is generally believed to be the cross-linked tyrosine, which then forms a neutral radical.[162,163] This notion is indirectly supported by the mentioned FTIR data[161] because a tyrosine radical cation seems highly unlikely. A recent X-ray structure of the reduced C*c*O from *Rh. sphaeroides*[141] shows water molecules between the cross-linked tyrosine (Tyr-288 in *sphaeroides* C*c*O) and the expected location of O_2 bound to heme iron, providing an excellent pathway for the proton required in the reaction. Interestingly, the corresponding structure of the oxidized C*c*O lacks these water molecules.[141]

Blomberg et al.[164,165] studied the O−O bond scission in C*c*O by quantum-chemical methods. As expected from previous work on other hemoproteins, they found that the oxygen adduct (Compound A) is an open shell singlet state with antiferromagnetic coupling between ferric heme iron and bound superoxide (Figure 6). Next follows simultaneous transfer of a proton from Tyr-244 to the distal oxygen atom and of an electron from either Cu_B or the tyrosine to yield a ferric hydroperoxy intermediate en route to the P state(s), a reaction found to be endothermic by 10 kcal/mol. Then the O−O bond is cleaved with a barrier of *ca.* 10 kcal/mol.[164−166] Hence, the calculated activation barrier is altogether too high to account for the observed kinetics (see below). In contrast, Karpefors et al.[22] reported spectroscopic data on reaction rate versus temperature and found activation enthalpy ($\Delta H^{\ddagger}$) and entropy ($T\Delta S^{\ddagger}$) terms of 5.1 and −6.8 kcal/mol, respectively, for the reaction forming state P_M and similar data for P_R. The resultant free energy change of activation ($\Delta G^{\ddagger}$) of 11.9 kcal/mol is not far from the value expected based on the observed rate and transition state theory. Substituting D_2O for water yielded a KIE of ∼1.5[22,157] for both reactions, suggesting rate-limiting proton transfer, which together with the similar activation profiles is consistent with the idea that the rate-limiting step is formation of the hydroperoxy intermediate. The ∼6-fold difference in the rates of formation of P_R and P_M in the reaction of fully reduced and mixed-valence C*c*O with O_2, respectively,[156] may be viewed with this background. The difference between the two cases is that heme *a* is initially reduced in the P_R case but oxidized in the P_M case. Due to the anticooperative redox interaction between heme *a* and the BNC,[106] the redox potentials of the latter are expected to be *ca.* 120 mV more negative when heme *a* is reduced. Such an increase in the driving force may well result in the 6-fold difference in rates. This notion gains further support from the observation that the exceptional formation of a mix of the P_M and P_R states in a case where heme *a* remains mostly ferrous (in the Glu-242-Gln mutant, see below) is almost as fast as formation of P_R in the wild type enzyme.

To rationalize the very high reaction barrier obtained from the QM calculations (see above), Blomberg et al.[164−166] reasoned that an additional proton made available to the reactants, but not consumed, could lower the barrier sufficiently, and a proton in the so-called K-pathway was considered. However, mutating the key Lys-319 residue to Met in the K-pathway has only a very small effect on the kinetics of O−O bond scission,[161,167,168] making this alternative unlikely. It remains possible that the structural model currently used for the QM calculations, although recently enlarged considerably,[166] is still too small to quantitatively capture the energetics of O−O bond scission.

O_2 binding and bond splitting with formation of either the P_M or P_R state of the active site imply four-electron

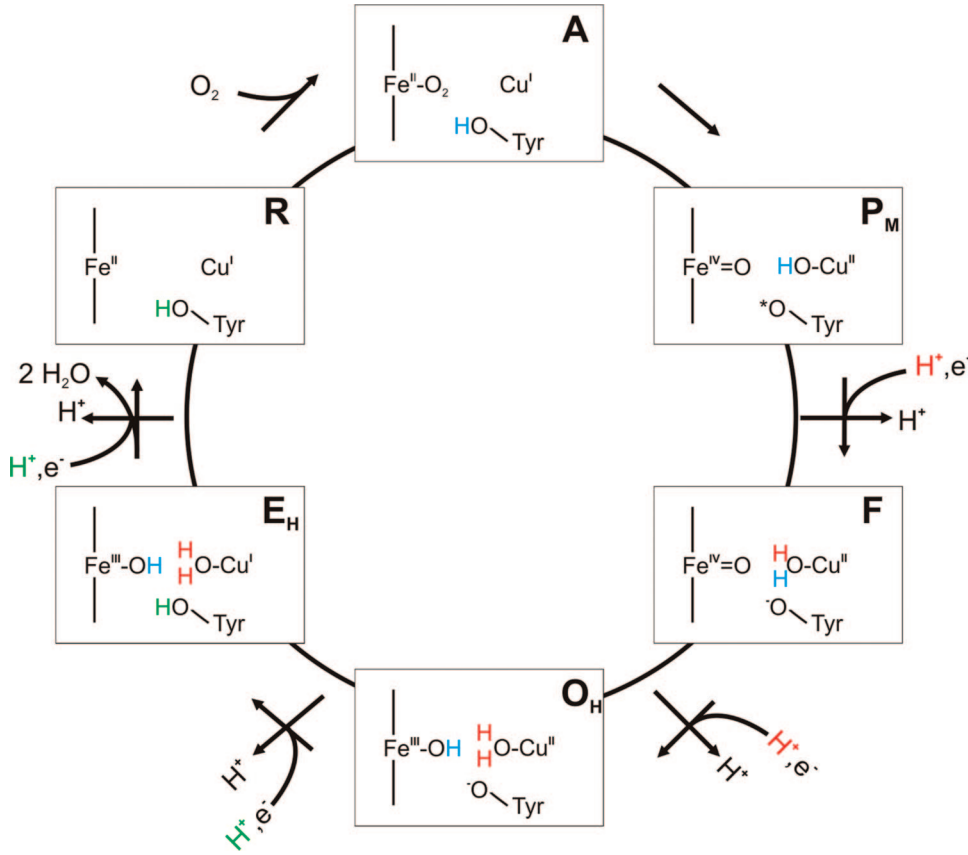

Figure 8. Catalytic cycle of C*c*O. Binding of dioxygen to the reduced ferrous/cuprous BNC (R) leads to formation of compound A followed by O−O bond scission that yields state P_M, after which four PCET reactions follow. In each of these four steps, a proton and electron are transferred from opposite sides of the membrane to the active site, in addition to translocation of one proton across the membrane. In the oxidative phase of the cycle (P → O), the chemical protons derive from the D-channel (red H^+), whereas in the reductive phase (O → R), the chemical protons are taken up from the K-channel (green H^+).

Table 2. $E_{m,7}$ Values and Driving Forces in the Catalytic Cycle of C*c*O[a]

	$E_{m,7}$ (mV)	$-\Delta G'_0$ (eV)
$P_M \rightarrow F$	817[b]	0.52
$F \rightarrow O$	762[b]	0.46
$O \rightarrow E$	<400[c]	0.10
$E \rightarrow R$	<400[c]	0.10
$R \rightarrow A$	0[d]	
$A \rightarrow P_M$		0.22[e]
sum of driving forces		1.40
expected sum of driving forces (800 mV to 300 mV) × 4		2.0
shortfall		0.60

[a] The driving forces (pH = 7) assume a potential of 300 mV for the electron donor, cytochrome *c*, and one of 800 mV for the O_2/H_2O couple (see text). [b] Values from redox titrations in mitochondria at high proton motive force, corrected to zero proton motive force and pH = 7.[169] [c] Maximal $E_{m,7}$ values observed in anaerobic redox titrations.[106] [d] See refs 144, 146, and 147. [e] See refs 164 and 165.

reduction of dioxygen all the way to the equivalent of water, avoiding the reactive oxygen intermediates (Table 1). QM calculations indicate that the reaction step A → P_M is exergonic by ~5 kcal/mol (the binding of O_2 being almost isoergonic, as indicated above).[164,165] In this reaction, the oxidizing power of O_2 is transferred to the active site of C*c*O, where the ferryl heme and the neutral tyrosine radical in the P_M state each have redox potentials of *ca.* 0.8 V, *i.e.* near the mean value for O_2 reduction to water in solution (Tables 1 and 2).

4.2. Intermediate States of the Binuclear Center

4.2.1. States P_M, P_R, and F

The P_M structure described above with a ferryl heme and a neutral radical is analogous to the classical "Compounds I" of, for example, peroxidases, catalases, and cytochrome P450[170−172] with the exception of the location of the radical. Addition of one electron to Compound I yields Compound II, which still has a heme ferryl structure but where the radical is reduced. In C*c*O there are two forms of "Compound II", viz. the P_R and F states of the binuclear site, which differ by one more proton in the latter. The optical spectra of these two states are very different in the α-band, which was part of the reason for the erroneous belief that both could not have ferryl hemes.[149] It seems likely that the extra proton in F (relative to P_R) forms a water molecule as the fourth ligand of Cu_B[II] instead of OH^- (Figure 8). An aquo ligand on the copper could donate a hydrogen bond to the oxo ligand of the ferryl heme, making the heme less axially symmetric, which could modify the α-band spectrum. The only reasonable alternative proton-accepting site in F would be Tyr-244, but that is contrary to FTIR evidence that this residue is anionic in the F state.[161,173] A curiosity is worth mentioning here. The aberrant ba_3 heme−copper oxidase from *Th. thermophilus* forms an F intermediate, but in this case, it has the same optical spectroscopic features as P,[174] which suggests that the cross-linked tyrosine is the proton acceptor in the P to F transition rather than Cu_B−OH (Figure 8). Interestingly, the P → F transition of the *Th. thermophilus* C*c*O is not coupled to proton translocation.[174]

After the P_M state, the catalytic cycle continues with four reaction steps, in each of which an electron and a proton are transferred to the BNC, and an additional proton is translocated across the membrane (Figure 8).[120,175] The P_R state is unique in the sense that it is the only experimentally observed form of the BNC in which an electron has been accepted by the center without a proton in the BNC proper; P_R accumulates transiently in the reaction of the fully reduced enzyme with O_2 (see above), and its status is of particular interest with respect to the function of the proton pump (section 5.3).

The rates of the consecutive steps P → F and F → O during the reaction of the fully reduced C*c*O with O_2 vary somewhat depending on the source of enzyme, but we may quote generic values of the time constants to be $\tau \sim 100\ \mu$s and 1 ms, respectively, i.e. roughly a 10-fold difference. Both transitions are known to involve transfer of an electron and a proton to the BNC, and to be coupled to transfer of another proton across the membrane (pumping; Figure 8). Since the proton pump mechanism is generally assumed to be the same in all four pump transitions, and since both reactions involve eT from heme *a* to the BNC and pT from the N-side to the BNC, the question arises why the F → O transition is so much slower than P → F. Figure 3 may help to provide the answer. It seems clear that in C*c*O the electron tunneling between heme *a* and the BNC is never itself rate-limiting (section 3.3) but that all PCET is controlled by protons.[156] PCET in connection with loading of the pumped proton will be discussed below (section 5), and we now consider the proton transfer in Figure 3 to denote uptake of the substrate proton, and we hence, assume that the proton-loading site (PLS) has been loaded with the pumped proton (section 5). After loading the PLS, there is a quasi-equilibrium with respect to eT between heme *a* and the BNC (states OX and RED, Figure 3). The overall rate of the final transition is determined by the subsequent rate-limiting proton transfer. Therefore,

$$\upsilon = k_{pT}[\mathrm{RED}] \quad (7)$$

where k_{pT} is the rate constant of proton transfer and [RED] is the occupancy of the state where the binuclear center is reduced and the PLS is loaded. The P → F transition is unique in the catalytic cycle (when starting from fully reduced enzyme) in that state P_R (= RED in Figure 3) is highly occupied, which implies that the observed rate ($\sim$10,000 s^{-1}) is close to k_{pT}. The equivalent RED state in the F → O transition has a much lower occupancy and has not been observed experimentally, which can easily explain the 10-fold slower rate.

The F state of C*c*O relaxes into the ferric cupric form (O), which is the oxidoreduction state of the BNC in the isolated enzyme (Figure 8; but see section 4.2.2). Wiertz et al.[176] detected an EPR signal in rapid freeze−quench experiments of the C*c*O reaction with O_2 that they originally assigned to a tryptophan cation radical in the P_M state. However, in later work using Q-band EPR spectroscopy,[177] this species was reassigned as the neutral radical form of Trp-236 (Trp-272 in C*c*O from *P. denitrificans*). Maximal occupancy of the radical ($\sim$5%) roughly coincided in time with maximal occupancy of the F state. The radical was proposed to be the result of electron transfer from Trp-236 to the BNC and to belong to an intermediate in the conversion of F to O.[177] Trp-236 is an interesting completely conserved residue that forms a π-stacking interaction with the His-291 ligand of Cu_B. To us it remains possible that the observed Trp-236 radical is indeed the result of eT from Trp-236 to Fe[IV]═O^{2-}, or more likely to Cu_B[II], as proposed,[177] but that it is an isoelectronic minority form of the F state in rapid equilibrium with the major form Fe[IV]═O^{2-} Cu[II]−OH_2 (Figure 8). If so, the 5% shift of electron density from Trp-236 to Cu_B in the F state would support the notion that the redox potential of Cu_B is far higher during turnover than what is measured in anaerobic redox titrations (see section 4.2.2).

The decay of the F state into state O occurs via a transient state where the ferric heme a_3 has a distal hydoxide ligand, sometimes called state H.[178,179]

4.2.2. Metastable States of the Binuclear Center

It was recognized early on that the ferric/cupric enzyme can exist in different forms, named "resting" versus "pulsed" and "slow" versus "fast".[180−182] Very generally, the ferric/cupric enzyme, as isolated, exhibits slow eT and ligand binding kinetics that may be accelerated considerably by enzyme reduction and reoxidation with O_2 ("pulsing"). The interest in this phenomenon was revived when it was reported that the reductive phase of the catalytic cycle (O → E → R; Figure 8) was linked to proton translocation only if immediately preceded by an oxidative phase (R → O), i.e. by oxygen pulsing.[120,175] State O of the binuclear site was consequently postulated to exist in a metastable state (O_H) during turnover that relaxes to a low-energy O state on exhaustion of electron donors. So far, no spectroscopic difference between these states has been found,[183] but the time-resolved data reported by Belevich et al.[119] clearly showed that the midpoint redox potential of Cu_B in the O_H state must be at least 100 mV higher than that observed in equilibrium redox titrations[184] (see also refs in ref 106). Analysis of the thermodynamics of the catalytic cycle (Table 2) shows that there is a shortfall of at least 0.6 eV (13.8 kcal/mol) in the sum of driving forces of the individual reaction steps, relative to the overall driving force. This provides independent evidence for the notion that the redox properties of either or both intermediates O and E, as deduced from anaerobic equilibrium titrations, are not applicable to the functioning catalytic cycle where these intermediates attain metastable states with higher redox potentials. This conclusion is consistent with the experimental observations that prior oxygen pulsing was necessary in order to observe proton-pumping coupled to reduction of the O state (see above). The structural basis of the pulsed O_H state relative to O is still not understood, but it has been speculated that lack of turnover may cause loss of water molecules from the cavity above Glu-242 (see section 5.1).

4.2.3. Bridging Ligand in the Binuclear Site

It has long been recognized that ferric heme a_3 and cupric Cu_B of the BNC are magnetically coupled in the oxidized enzyme, quenching EPR signatures from both paramagnets. Early X-ray structures showed electron density between the metals that was interpreted as two oxygenous ligands, for example a hydroxide at Cu_B and water at heme iron, or as a peroxide.[11] Recent improvement of resolution has strengthened the latter interpretation, and two groups have independently proposed that the bridging ligand is a peroxide dianion.[139,140] Kim et al.[185] criticized the original peroxide proposal on the basis of the structural properties of model

compounds with peroxide bridging between the metals, and they proposed that the intermetal electron density may even be bound dioxygen. This suggestion has recently gained support from quantum-chemical calculations (Kaila et al., submitted) which indicate that the best fit of the bound ligand is superoxide that might have been formed in the site from bound O_2 due to the X-ray irradiation.

5. Proton Pumping

5.1. Proton Transfer Pathways

The D- and K-pathways of proton uptake from the N-side of the membrane were already briefly introduced (Figure 1). The D-pathway has been extensively studied by both mutational and computational methodologies (see, e.g., ref 186 and references therein). It starts at Asp-91 and ends at Glu-242 in the middle of the membrane domain *ca.* 10 Å from the binuclear site. Beyond Glu-242, there is an apolar cavity that has been predicted to at least transiently contain water molecules[187−191] and which during turnover might actually be continuously filled by water produced as the product of the chemistry at the BNC. The existence of water molecules in the apolar cavity seems to be demanded by the structure, because in their absence it would be virtually impossible to imagine how protons are transferred further from Glu-242 to the PLS or to the binuclear center, the latter at a distance of ∼10 Å from Glu-242. The D-channel proper contains several water molecules that are seen in the crystal structures with very little positional variations, and conserved polar amino acids that line the pathway. Henry et al.[186] showed by free energy calculations that the D-channel as captured in the crystal structures is not a continuous pT "wire" but is interrupted at the Asn-98, so that a side chain isomerization of this residue is required to gate protons along the pathway. Many mutations in D-pathway residues have been reported to decouple the proton pump, i.e. decrease or abolish the stoichiometric efficiency of proton-pumping with far less inhibitory effect on turnover (for a summary, see ref 186). In some cases where asparagine residues in the channel have been replaced by aspartate, turnover has been reported to be unaffected or even increased, but proton-pumping was abolished.[192] The original explanation for this effect was an electrostatic perturbation of the pK_a of the key residue Glu-242, which would make pT from this residue to the PLS unfavorable.[193] However, replacements of the asparagine by neutral residues yield similar effects (see ref 186), and the most likely cause for the defect is compromised kinetics of reprotonation of Glu-242.[4,186,194]

According to recent theoretical studies[195,196] (but contrast ref 74), slower reprotonation kinetics of Glu-242 could lead to an increased population of the anionic Glu-242 with contact to the pump site (PLS), a state vulnerable to proton leaks. This is supported by the crystal structure of the Asn98Asp mutant enzyme, in which the side-chain of Glu-242 has rotated to a conformation pointing toward the P-side.[194] Uncoupling of proton-pumping from oxygen reduction in such mutants could take place by back leakage of the proton at the pump site when the BNC is reduced and protonated.

The key residue of the K-pathway is Lys-319, and the channel seems to lead to the cross-linked tyrosine of the binuclear site. In contrast to the D-channel, there are few water molecules in the K-channel and no continuous pT "wire" is observed. Mutating the Lys-319 does not appreciably affect the oxidative phase of the catalytic cycle but effectively blocks reduction of the BNC.[197−199] It has been deduced, therefore, that the K-channel only conducts the chemical protons of the reductive phase of the catalytic cycle, where the ferric/cupric binuclear site is being reduced (section 4). It was uncertain for some time whether the K-channel is a true proton transfer pathway. However, this function was ascertained by the observations that, after photolysis of CO from reduced heme a_3 at high pH, the eT from heme a_3 back to heme *a* is associated with proton release from the binuclear center, which is blocked in the Lys319Met variant but not in mutants of the D-pathway (section 3.3).

5.2. PCET and Proton Pumping

According to current knowledge, the catalytic cycle of C*c*O encompasses four reactions, in each of which electron transfer to the oxygen reduction site is coupled to translocation of one ("physical") proton from the N- to the P-side of the membrane[120,175] (Figure 1). Each of these reactions also includes uptake of another ("chemical") proton into the BNC to complete the chemistry of water formation. While the chemistry at the BNC is different in the four reaction steps, it has been generally assumed that the mechanism of proton-pumping is essentially the same in each step, as most recently pointed out by Fadda et al.[71] The major proposed mechanistic sequence of proton-pumping is based on the notion[200,201] that it is the uptake of the "chemical" proton into the BNC that drives out a "prepumped" proton from a proton-loading site (PLS) into the P-phase. Fadda et al.[71] eloquently described the basics of this sequence of events (see also refs 4, 66, 119, 169, 190, 195, 202−204), which may briefly be summarized as follows (Figure 9):

(1) A proton-loading site (PLS), presumably located at or near the A-ring propionate of heme a_3,[205] receives a proton from the N-phase (via Glu-242) when the electron resides at the electron-queuing site, heme *a*, which has raised the pK_a of the PLS.

(2) The proton in the PLS raises the redox potential of the BNC, allowing eT from heme *a* to this site, which occurs with the same kinetics as the loading of the PLS.

(3) The electron in the BNC attracts a "chemical" proton more than it attracts the proton in the PLS (shorter electron/proton distance). Consequently, a proton is taken up from the N-side into the BNC, and this expels the proton from the PLS into the P-phase by electrostatic repulsion.

(4) New electron density is transferred from Cu_A to heme *a*.

It is noteworthy that for this mechanistic principle to function, step 1 of the above sequence demands heme *a* to be close to the PLS, while steps 2 and 3 demand the PLS to be close to the binuclear center (BNC).

This electrostatic mechanism gained considerable support from time-resolved experiments in which C*c*O in the O_H state was photoinjected with an electron and the electron and proton trajectories were followed in real time by spectroscopic and electrometric techniques.[119] The results from this work have subsequently been analyzed and discussed in detail, yielding estimates of the pK_a values of the PLS (Figure 9B), redox potentials of the metal centers, equilibrium constants, and reaction barriers for the different stages of the proton pump reaction.[4,204] However, the mechanism as described above and in Figure 9B is incomplete, because it fails to address the fundamental problem of any pump, *viz.*

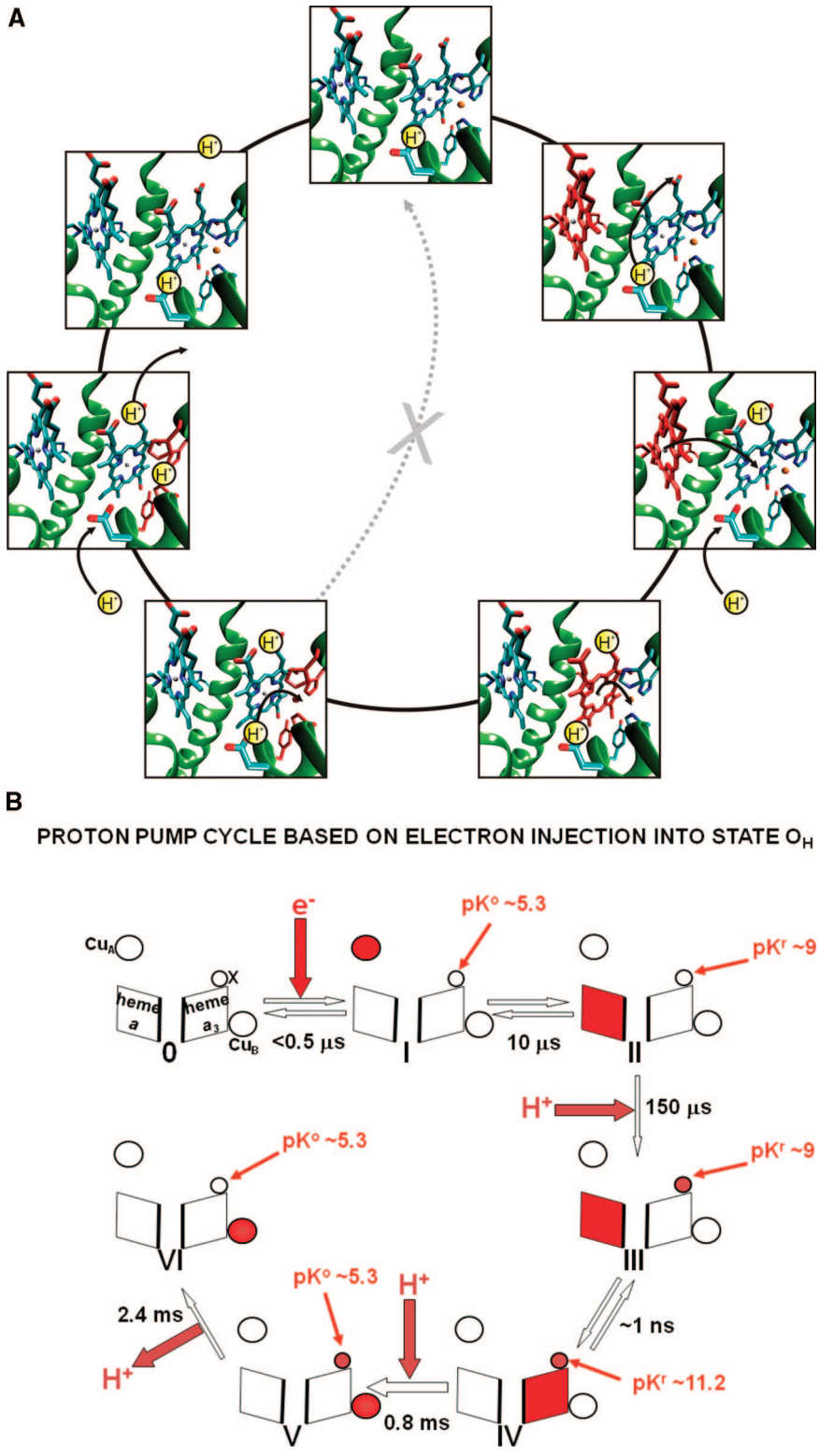

Figure 9. Proton-pumping mechanism. (A) From upper corner clockwise. An electron arrives at heme *a*, causing pT from Glu-242 to the pump-site within 150 μs (here: A-propionate of heme a_3). Protonation of the pump-site increases the midpoint potential of heme a_3, which leads to eT within 1.2 ns. After reprotonation of Glu-242 from the D-channel, the proton of Glu-242 is transferred to the reduced BNC due to its increased proton affinity. After reprotonation of Glu-242, the proton at the pump-site is repelled to the P-side of the membrane within 2.6 ms. (B) Scheme of the pump mechanism with experimentally evaluated rate and equilibrium parameters.

how its directionality is secured. The molecular nature of leak prevention by gating of the C*c*O proton pump has been addressed only relatively recently, in the analysis of the time-resolved experimental data[4,204] and in mathematical modeling of the minimal prerequisites of such a pump mechanism.[206,207] Major potential leaks may be addressed as follows, using the scheme of Figure 9B as a reference:

Transfer of a proton to the PLS from the P-side of the membrane rather than from the N-side in the reaction II → III would obviously short-circuit the pump. This leak is analogous to the "back-reaction" VI → V (Figure 9B), the activation barrier of which has been deduced to be 16.0−16.7 kcal/mol,[4,195,204] corresponding to a time constant of slightly above 100 ms based on standard transition state theory. This

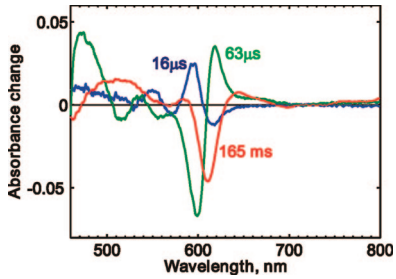

Figure 10. Reaction of the Glu-242-Gln variant enzyme with O_2. Flow-flash measurement with the Glu-278-Gln mutant of C*c*O from *P. denitrificans*, as described previously.[161] Syringe 1: 12 μM enzyme, 200 mM MOPS buffer (pH 7.0), 0.05% dodecylmaltoside (DDM), 2 μM *N,N,N′,N′*-tetramethyl-*p*-phenylene diamine (TMPD), 4 mM sodium ascorbate, 1 atm of CO; syringe 2: 200 mM MOPS (pH 7.0), 0.05% DDM, 1 atm of O_2. The reaction starts with a laser pulse (BrilliantB; Quantel, Les Ulis, France; frequency-doubled YAG, 532 nm, pulse energy 80 mJ, pulse duration 4 ns). The difference spectra of three time-resolved reaction phases are shown together with their respective time constants (inverse rate constants).

leak is thus slow enough relative to the rates in the normal sequence not to compromise the efficiency of the pump. Yet, it is of substantial interest in terms of the general design of the proton pump mechanism. If, following the scheme in Figure 9B, the forward step V → VI were much faster with a correspondingly much lower barrier of activation but with the same change in free energy, then the barrier of the back-reaction VI → V would be lower as well, so that the rate of the leak reaction could easily become substantial. The fact that the pumped proton is released relatively slowly in the step V → VI is therefore an important mechanistic detail in the design of an efficient pump, but the molecular basis for why this reaction is slow is not yet understood. This scenario predicts that if normal proton transfer from the N-side is prevented, for example by mutating Glu-242 to Gln, then a delayed reaction II → III might be observed with a time constant of ~100 ms or slightly above, due to proton leak from the P-side to the PLS. Such a leak reaction may most easily be observed as a delayed (≥100 ms) electron transfer phase from heme *a* to the BNC (*i.e.* reaction III → IV) coupled to the erroneous protonation of the PLS.

Figure 10 shows the results of such an experiment with the Glu-278-Gln variant of C*c*O from *P. denitirificans* (homologous to Glu-242-Gln in the bovine enzyme). Flashing off CO from the fully reduced enzyme allows the reaction with added O_2 to start. The 16 μs phase shows the spectrum typical of the oxygen adduct (state A). The next phase (τ = 63 μs) has a spectrum typical of formation of the P intermediate. A key issue is whether it is the P_M or the P_R state that is formed here, with the only difference being whether heme *a* becomes oxidized (P_R) or not (P_M). In the reaction of the fully reduced wild type enzyme with O_2, the product is exclusively P_R (see section 5.3), and this fact may have biased previous interpretations of experiments such as the one in Figure 10 to conclude that the P_R state is formed exclusively also in the oxygen reaction of the Glu242Gln variant.[161,208] However, careful analysis of the spectrum of the 63 μs (53 μs in ref 161) reaction phase shows only ~30% oxidation of heme *a*; hence, on this time scale, P_R is formed to 30%, with the rest being P_M. Note also that, in the Glu-242-Gln variant, the P intermediates are formed about three times faster than P_M is formed when mixed valence enzyme reacts with O_2, presumably due to the initially reduced state of heme *a* (see section 4.1).

The 30% oxidation of heme *a* (and formation of P_R) at the P stage in the Glu-242-Gln variant, *i.e.* without compensation of the eT by pT, is clearly a potential leak reaction and shows that the E_m of the neutral tyrosine radical/tyrosinate electron acceptor couple is only some 20 mV more negative than that of the donor, heme *a* ($E_m \sim 270$ mV[4]), when the electron is uncompensated by a proton at the PLS or at the BNC itself. This is different from the case during the $O_H \rightarrow E_H$ transition, where premature eT into the BNC to generate a potential leak was found to be less than 1%[4,119] and shows that the tyrosine radical is relatively highly oxidizing even without protonation.

Formation of P_R in fully reduced WT enzyme is at least two times faster than formation of the P states in the Glu-242-Gln variant.[203] Thus, the faster kinetics of the PCET with protonation of the PLS, compared to eT alone, favors the coupled path by 67% vs 33%. Moreover, as discussed above (Figure 10), only ~$^1/_3$ of the noncoupled eT occurs from heme *a* (the rest occurs from the tyrosine forming the P_M state) so that maximally only ca. 10% of the encounters of the fully reduced wild type enzyme with O_2 will lead to loss of proton-pumping. Here it should be further recalled that the fully reduced enzyme is, as such, a very improbable state during turnover under physiological conditions.[2]

Most importantly, Figure 10 also shows a 165 ms phase in the reaction of the Glu-242-Gln variant with O_2 that went previously unnoticed[161] because the time-resolved spectroscopy equipment did not extend beyond 2 ms. This phase consists purely of oxidation of the remaining 70% of heme *a* within the population of enzyme that reacted with oxygen and formed state P_M in the 60 μs reaction. No other spectral changes are observed for this phase, so it represents delayed electron transfer from heme *a* into the P_M state of the BNC, which is precisely the behavior expected due to leak of a proton from the P-side of the membrane into the PLS (see above).

While the mechanistic sequence explains the release of the proton in the PLS in the reaction V → VI, it fails to explain why it is ejected to the P-side of the membrane rather than to the N-side (Figure 9B), which would be energetically more favorable in the presence of proton motive force. It has been pointed out[4,204] that the kinetic barrier for pT from the N-side of the membrane to the PLS must be substantially lowered by the electron at heme *a* (as in state II, Figure 9B) and consequently high enough to prevent proton backflux when heme *a* is oxidized (as in state V). Interestingly, precisely such gating of pT by the position of the electron was found necessary in purely mathematical modeling of the proton pump mechanism,[207] and different molecular explanations for such gating have been discussed.[4,190,195,204,209]

Our next example of potential leak relates to the possibilities of premature PCET to the BNC in state II (Figure 9B). Primary eT followed by pT was already discussed above for the special case of the fully reduced enzyme. In other cases, it is prevented by the even more thermodynamically unfavorable eT into the BNC when not charge-compensated.[4,204] Premature pT followed by eT (Figure 3) would most likely be limited by pT to the BNC that would occur prematurely with the electron still at heme *a*. Such PCET leading to leakage has been discussed[4,204] and may be prevented by a sufficiently high barrier against forming a competent pT pathway from Glu-242 to the BNC by water molecules.[190]

While a basic electrostatic mechanism is widely agreed upon, with only relatively small variations (see refs above),

there are two fundamentally different mechanistic proposals, one by Brzezinski and Larsson[210] and another by Yoshikawa et al.[11,132] In the former, the sequence of events is interchanged from the above in an important way. Thus, transfer of the chemical proton to the BNC occurs first and leads to a conformationally strained state with pK_a values that secondarily drive the pumped proton to the PLS (see section 5.6). The latter mechanism is yet very different and even involves a pT pathway different from those discussed here. Perhaps the major dilemma with the Yoshikawa mechanism is that if it is correct, it would have to be unique for mitochondrial C*c*O, whereas the majority belief at this point is that the mitochondrial and bacterial C*c*O mechanisms probably are very similar. A thorough discussion of both these mechanisms has been published.[4]

While the major experimental basis of the electrostatic mechanism derives from electron photoinjection experiments,[119] the Brzezinski−Larsson mechanism (see also section 5.6) is largely based on experiments where the first proton-pumping step has been studied after the fully reduced C*c*O reacts with O_2,[210] *viz.* the transition from the A state of the binuclear site to form the F state via P_R (section 4). Although the common belief is that all proton-pumping steps are mechanistically equal in principle[211] (see also above), there are distinct differences between these two reaction steps that require deeper analysis (section 5.3).

5.3. Proton Pumping via the P_R State

It was thought early on[2] that proton pumping might be initially short-circuited in the reaction of the fully reduced enzyme with O_2, a reaction that hardly occurs in physiological steady states. However, it has been convincingly demonstrated[212,213] that the reaction sequence R → A → P_R → F is linked to proton pumping, as it is, for example, in the step F → O (Figure 8). Yet, the early reactions of the fully reduced enzyme with O_2 appear anomalous from several points of view, especially when compared to the sequence of events deduced from experiments where the O_H state is photoinjected with an electron[4,119,203] (section 5.2). For example, the former occurs very much faster than the latter. Belevich et al.[203] reported that the reaction step A → P_R occurs by the same kinetics as the initiation of the proton pump sequence by loading of the PLS with a proton. This observation of PCET is of fundamental mechanistic significance because it provides an explanation for the apparent violation of Peter Rich's electroneutrality principle for the binuclear site,[214] as the eT is not accompanied by pT into the BNC during A → P_R. Glu-242 was identified as the proton donor, since the electrometric response attributed to protonation of the PLS was abolished in the Glu-242-Gln variant. However, the expected tight coupling between this proton transfer and electron transfer from heme *a* to the BNC forming the P_R intermediate seemed to be at variance with previous reports according to which the P_R state would be readily formed in the Glu-242-Gln variant and at almost the same rate as in wild type enzyme.[161,208] But, as already suspected[169] (*cf.* section 5.2 and Figure 10), the product of the oxygen reaction in the Glu-242-Gln mutant is not the pure P_R state with full eT from heme *a* to the BNC but rather a state dominated to 70% by P_M. In other words, blocking the pT from Glu-242 to the PLS considerably diminishes the extent of eT from heme *a* to the BNC on the submillisecond time scale. The P_M and P_R states may be envisioned by Figure 3, in which the OX/RED couple would now be the Tyr-O*/Tyr-O$^-$ pair of the cross-linked tyrosine in the active site. The corresponding redox potentials of the tyrosine radical/tyrosinate and for the phenol radical/phenolate pairs are 0.68[215] and 0.87 V[216] in aqueous solution, respectively, and the latter is raised to 0.94 V when the phenol is cross-linked in the ortho position with imidazole.[216] The high redox potential would *a priori* be expected to lead to complete eT from heme *a* to Tyr-O* and formation of P_R in the Glu-242-Gln variant. Instead, we observe 30% heme *a* oxidation on the fast time scale (Figure 10), indicating an E_m value of the P_M/P_R couple of ∼250 mV (section 5.2). However, the overall charge of the BNC in the mutant is one unit more negative in P_R than in P_M, and such addition of uncompensated charge represents work against the principle of electroneutrality of the oxygen reduction site.[214] The energy cost of inserting a charge with radius r into an apolar domain with a dielectric constant of ε may be estimated from

$$\Delta G = \frac{N_A q^2 e^2}{8\pi\varepsilon\varepsilon_0 r} \tag{8}$$

where N_A is Avogadro's number, ε_0 is the permittivity of vacuum, e is the charge of the electron, and q is the number of charges[217] (note that in refs 214 and 215 a factor of 2 is lacking in the denominator). Inserting the constants yields,

$$\Delta G = \frac{7.2}{\varepsilon r} \tag{9}$$

where ΔG is expressed in eV and r in ångströms. Assuming a value of 3 Å for the radius of the charge in the tyrosinate anion and a Born penalty of 0.43−0.69 eV (using the extreme potentials of the "model tyrosines" and 0.25 V for the P_M/P_R couple, as discussed above) yields $\varepsilon = 3.5-5.6$, quite reasonable values for the protein interior. Although this approximation is rough, it helps to point out once more that eT from heme *a* to the BNC is usually quite unfavorable thermodynamically unless charge-compensated. In the special case of the neutral tyrosine radical here, such eT was observed only due to its very high electron affinity, which remains measurable even in the absence of charge compensation.

5.4. Is the Proton-Loading Site "Loaded" in the Fully Reduced Enzyme?

In the electrostatic proton pump mechanism (section 5.2), the proton-loading site (PLS) is protonated as a response to reduction of heme *a*, which raises the pK_a of the PLS from *ca.* 5 to 9−11.[4,195,204,218] In the fully reduced enzyme, the electrons in the binuclear center are charge-compensated by protonation,[214] so that the overall charge of the BNC should be the same as in the oxidized C*c*O. The reduced state of heme *a* would therefore *a priori* be expected to ensure protonation of the PLS. However, as will be discussed below, there is strong experimental evidence to the contrary, *viz.* that the PLS is unoccupied in the fully reduced enzyme.

Reduction of the binuclear site (two electrons) is associated with net uptake of two protons,[219] but further reduction of heme *a* (plus Cu_A) is linked to net uptake of not more than ∼0.4 protons.[219,220] Moreover, the latter proton uptake takes place from the P-side of the membrane. Mitchell and Rich[219] showed that oxidation of the fully reduced bovine heart enzyme by O_2 is coupled to net uptake of ∼1.6 protons, and we have verified this observation (I. Belevich et al., unpublished). Since 4.0 protons must be consumed overall

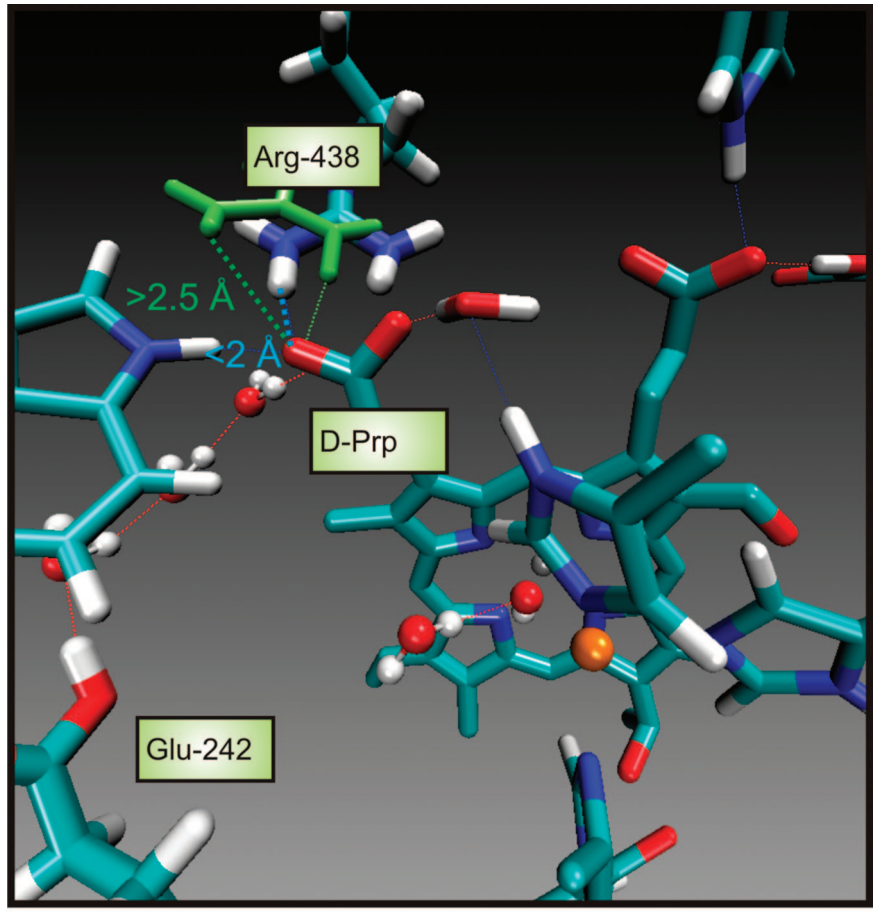

Figure 11. Dissociation of Arg-438 and the D-propionate of heme a_3 obtained from 5 ns MD simulation of C*c*O in a state with heme *a* reduced and the BNC in the P_M state, simulating a proton-pumping step as discussed previously.[224−226] Here, the simulation was performed using NAMD,[227] our in-house parametrization of redox-active groups,[107] and the CHARMM27 force field.[228]

on enzyme oxidation by O_2 followed by rereduction (because $4e^- + 4H^+ + O_2 \rightarrow 2H_2O$), full reduction must be coupled to uptake of $\sim 2.4H^+$, which has been confirmed by direct measurements by Forte et al.[221] and by Parul et al.[222] One proton each is known to be consumed in the P → F and F → O transitions.[223] The observed overall consumption of $1.6H^+$ on oxidation by O_2 is therefore expected, since reoxidation of heme *a* plus Cu_A causes release of $\sim 0.4H^+$ (see above).

This data definitely excludes a loaded PLS in the fully reduced enzyme. If the PLS were protonated, oxidation of the fully reduced enzyme with O_2 would cause release of that proton, resulting in net uptake of only 0.6 H^+. Furthermore, time-resolved electrometric data suggest pT from Glu-242 to the PLS during the A → P_R reaction (see above[203]). Finally, if the PLS were preloaded in the fully reduced enzyme, the overall electrical work during A → P_R → F should be considerably less than during F → O, which is not the case, as shown by electrometric experiments.[119]

We conclude that the pK_a of the PLS must be well below 7 in the fully reduced enzyme, contrary to what would *a priori* be expected on the basis of the proton pump mechanism (section 5.2). The notion in that mechanism that reduction of heme *a* leads to a rise in pK_a and protonation of the PLS is based on experiments where an electron is photoinjected into C*c*O in the O_H state.[119] In contrast, electron injection to enzyme in the relaxed O state (*i.e.* the oxidized enzyme as isolated; see section 4.2.2) also fails to cause loading of the PLS despite the fact that heme *a* is reduced.[120] The property of the PLS in the fully reduced C*c*O is thus no different from that in state O. Neither state participates in the catalytic cycle.

5.5. Gating Protons by Electrons

The electrostatic proton pump mechanism presented in section 5.2 has been supported by molecular dynamics simulations. The simulations showed formation of a "proton wire" of water molecules between Glu-242 and the D-propionate of heme a_3 specifically when heme *a* was reduced and the BNC oxidized, *i.e.* prior to eT to the BNC. Moreover, in simulations of this redox state, the D-propionate/Arg-438 ion pair dissociates transiently, which makes the propionate accessible for protonation[53,224−226] (Figure 11). In this redox state, no such proton transfer path was formed between Glu-242 and the oxygen reduction site (Figure 12[190]). Reduction of the BNC by eT from heme *a* altered the dynamics of the water molecules in the nonpolar cavity above Glu-242 so that now a proton wire readily formed between the Glu-242 and the OH^- ligand of Cu_B (Figure 12).[190] For such a "water-gated" mechanism to function, there must be a sufficiently high kinetic barrier against short-circuiting reactions, *e.g.* against forming a proton wire from Glu-242 to the BNC, prior to loading the PLS and the eT from heme *a* to the BNC. Such control is unlikely to be solely based on different orientations of water chains, as thought originally,[190] but probably also depends on control of water occupancy in the different domains of the nonpolar cavity by the electric field created by the redox reaction (see sections 2.2 and 5.2 and below).

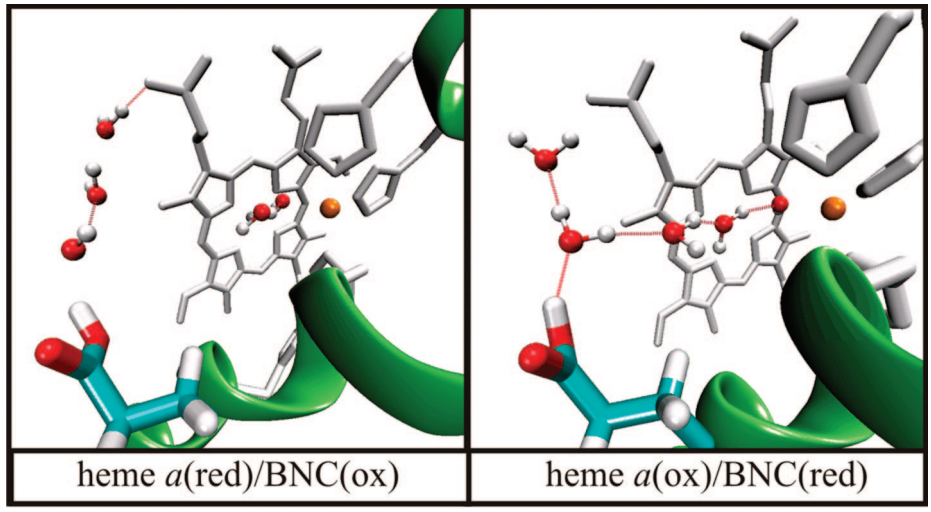

Figure 12. Formation of redox-state dependent proton wires in the nonpolar cavity above Glu-242. When heme *a* is reduced and the BNC is oxidized (here state P_M), a proton wire is formed between Glu 242 and the D-propionate of heme a_3 but not to the BNC. Upon transfer of the electron to the BNC (forming the P_R state), a proton wire is formed between Glu-242 and the BNC. The simulation was performed using NAMD[226] and our in-house parametrization of redox-active groups[107] and the CHARMM27 force field.[227]

Pisliakov et al. stressed that the *energetics* of pT is not directly determined by the connectivity between donor and acceptor via water molecules but by the energetics of placing the water molecule into the structure and especially by the energetics of the pT from the donor to the first water molecule.[49] However, as discussed in section 2.2, the water wire orientates from proton donor to acceptor as a result of the local electric field in that domain, which is in turn modulated by the position of the electron density and, thus, controlled by the redox reaction. The rate-limiting energy barrier for transferring the proton into the wire is lowered considerably by the orientated water chain, due to the electric field created by the organized water dipoles (Figure 5B). The barrier is much higher with a single water molecule between donor and acceptor, since the charges in the transition state are more localized than those for a chain of water, and the dipole field is smaller. Therefore, the *energetics* of pT is in fact strongly favored by an organized chain of water molecules between donor and acceptor. Water polarization and proton conduction are intimately coupled. Due to the movement of the redox electron and the created electric field, there is a strong driving force on the proton to move to the proton acceptor site. For exactly the same reason, the water dipoles in the chain are polarized toward that site. Such behavior has, for example, been observed in combined first-principle/classical MD simulations of proton transfer in carbon nanotubes by Hassan et al.[90]

It is clear that the energetics of moving water molecules to a relatively nonpolar domain will contribute to the energetics of the pT process.[49] However, in C*c*O the water molecules in the nonpolar cavity above Glu-242 almost certainly stem from water produced as the product of the chemistry at the BNC nearby, so that the energy of moving water to this cavity from the bulk is irrelevant. The occupancy of water molecules in the different domains of this cavity is likely to be controlled by the electric field. eT to the BNC produces an electric field between Glu-242 and the BNC that draws water molecules into this domain (see section 2.2). This effect is analogous to the electroporation phenomenon,[98] where a proton-conducting water pathway is formed across a lipid membrane as a result of an electric field. Likewise, it is possible that filling the cavity between Asp-96 and the Schiff base in bacteriorhodopsin with four water molecules to aid pT from the former to the latter[229] is in part due to a change in the local electric field caused by deprotonation of the Schiff base.

5.6. An Alternative: Substrate Proton First, Pumped Proton Second

The driving force for moving the pumped proton in the Brzezinski−Larsson model[210] (see section 5.2), where it occurs secondarily after moving the substrate proton to the BNC, is generated quite differently from the model discussed above. The negative charge of Glu-242 generated by transfer of its proton to the BNC causes a "tense" conformation of the pump site (PLS) that increases its proton affinity. Although time-resolved experiments[119,203] and MD simulations[190] speak against this type of reaction mechanism, it is fruitful to consider the circumstances by which it could work. Here, the electron in heme *a* is transferred to the BNC without protonation of the pump site, and this is made possible by transferring a proton as well to the site from Glu-242. The produced anionic Glu-242 then increases the proton affinity of the pump site in a charged or tense configuration. However, as a new proton is taken up from the D-channel, it will pass through Glu-242, neutralizing its negative charge and abolishing the high proton affinity of the pump site. Such a mechanism could only work if relaxation of the high proton affinity of the pump site would be slower than the transient protonation of Glu-242. In that case, the high pK_a of the PLS could hardly be due to a purely electrostatic interaction with Glu-242, which would relax instantaneously. Another problem with this mechanism arises from proton pumping during the reductive phase of the catalytic cycle (see section 4.2.2). Here, the chemical proton is taken up from the K-channel[15,16,120] and, hence, no anionic Glu-242 is produced to drive uptake of the pumped proton.

6. Conclusions in Brief

Electrons tunnel in C*c*O from bound cytochrome *c* to the Cu_A site, and further to heme *a* into the membrane domain. Further eT from heme *a* to the binuclear site is strongly coupled to and controlled by protons. Protonation of a proton-loading site (PLS) in the propionate domain of heme a_3 is a

thermodynamic prerequisite for and controls this eT. A dipole is created with the positive and negative ends at the PLS and the BNC, respectively. The pumped proton is repelled from the PLS site to the aqueous P-side of the membrane by the electrostatic energy released when a chemical proton is taken up to fully neutralize the charge of the electron at the oxygen reduction site, effectively annihilating the charge separation in the dipole intermediate. The directionality of proton transfer is secured by gating the proton transfer pathway between Glu-242 and the PLS on the basis of the position of the electron density. This sequence is repeated four times during the catalytic cycle. The initial O−O bond scission at the active site leaves it with four "electron holes", which are filled sequentially in the subsequent four PCET reaction steps that are each coupled to proton pumping, followed by the binding of a new molecule of O_2.

The electric fields generated by eT between heme *a* and the oxygen reduction site direct the proton transfer reactions by polarizing and organizing functional water molecules into 1D chains within a nonpolar cavity in the protein structure. Electric field alteration between Glu-242 and the active site controls bifurcation of proton transfer either for proton-pumping or for oxygen reduction chemistry. Electric fields not only polarize water chains, but also affect their water occupancy, and hence their existence, and lower the kinetic barriers of proton transfer into those chains.

7. Abbreviations

BNC	binuclear center (active heme a_3-Cu_B site of C*c*O)
C*c*O	cytochrome *c* oxidase
DFT	density functional theory
$E_{m,7}$	midpoint redox potential at pH 7, relative to NHE
EPR	electron paramagnetic resonance (spectroscopy)
eT	electron transfer
FTIR	Fourier transform infrared (spectroscopy)
NHE	normal hydrogen electrode
KIE	kinetic isotope effect
K_M	Michaelis constant
MD	molecular dynamics
MM	molecular mechanics
PCET	proton coupled electron transfer
PLS	proton-loading site
pT	proton transfer
QM	quantum mechanics

8. Acknowledgments

The authors are indebted to Dr. Gerhard Hummer (NIDDK, NIH) for helpful discussions. This work was supported by grants from the Sigrid Jusèlius Foundation, Biocentrum Helsinki, and the Academy of Finland.

9. Note Added after ASAP Publication

There were errors in Table 1 in the versions published on 11/5/2010 and 11/19/2010. They were fixed in the version published on 12/8/2010.

10. References

(1) Mitchell, P. *Nature* **1961**, *191*, 141.
(2) Babcock, G. T.; Wikström, M. *Nature* **1992**, *356*, 301.
(3) Wikström, M. *Nature* **1977**, *266*, 271.
(4) Wikström, M.; Verkhovsky, M. I. *Biochim. Biophys. Acta* **2007**, *1767*, 1200.
(5) Wikström, M. *Biochim. Biophys. Acta* **2004**, *1655*, 241.
(6) Dutton, P. L.; Wilson, C.-P.; Lee, C.-P. *Biochemistry* **1970**, *9*, 5077.
(7) Tsukihara, T.; Shimokata, K.; Katayama, Y.; Shimada, H.; Muramoto, K.; Aoyama, H.; Mochizuki, M.; Shinzawa-Itoh, K.; Yamashita, E.; Yao, M.; Ishimura, Y.; Yoshikawa, S. *Proc. Natl. Acad. Sci. U.S.A.* **2003**, *100*, 15304.
(8) Humphrey, W.; Dalke, A.; Schulten, K. *J. Mol. Graphics* **1996**, *14*, 33.
(9) Sawyer, D. T. *Oxygen Chemistry*; Oxford University Press: 1991.
(10) Petlicki, J.; van de Ven, T. G. M. *J. Chem. Soc., Faraday Trans.* **1998**, *94*, 2763.
(11) Yoshikawa, S.; Shinzawa-Itoh, K.; Nakashima, R.; Yaono, R.; Yamashita, E.; Inoue, N.; Yao, M.; Fei, M. J.; Libeu, C. P.; Mizushima, T.; Yamaguchi, H.; Tomizaki, T.; Tsukihara, T. *Science* **1998**, *280*, 1723.
(12) Ndubuizu, O.; LaManna, J. C. *Antioxid. Redox Signaling* **2007**, *9*, 1207.
(13) Buse, G.; Soulimane, T.; Dewor, M.; Meyer, H. E.; Bluggel, M. *Protein Sci.* **1999**, *8*, 985.
(14) Bu, Y.; Cukier, R. I. J. *Phys. Chem. B* **2005**, *109*, 22013.
(15) Kaila, V. R. I.; Johansson, M. P.; Sundholm, D.; Laakkonen, L.; Wikström, M. *Biochim. Biophys. Acta* **2009**, *1787*, 221.
(16) Konstantinov, A. A.; Siletsky, S.; Mitchell, D.; Kaulen, A.; Gennis, R. B. *Proc. Natl. Acad. Sci. U.S.A.* **1997**, *94*, 9085.
(17) Gennis, R. B. *Front. Biosci.* **2004**, *9*, 581.
(18) Brzezinski, P. *Trends Biochem. Sci.* **2004**, *29*, 380.
(19) Huynh, M. H.; Meyer, T. J. *Chem. Rev.* **2007**, *107*, 5004.
(20) Knapp, M. J.; Rickert, K.; Klinman, J. P. *J. Am. Chem. Soc.* **2002**, *124*, 3865.
(21) Karpefors, M.; Ädelroth, P.; Brzezinski, P. *Biochemistry* **2000**, *39*, 5045.
(22) Karpefors, M.; Ädelroth, P.; Namslauer, A.; Zhen, Y.; Brzezinski, P. *Biochemistry* **2000**, *39*, 14664.
(23) Marcus, R. A. J. *Chem. Phys.* **1956**, *24*, 966.
(24) Marcus, R. A. J. *Chem. Phys.* **1956**, *24*, 979.
(25) Marcus, R. A. J. *Chem. Phys.* **1957**, *26*, 867.
(26) Marcus, R. A. J. *Chem. Phys.* **1957**, *26*, 872.
(27) Marcus, R. A.; Sutin, N. *Biochim. Biophys. Acta* **1985**, *811*, 265.
(28) Gamow, G. *Z. Phys.* **1928**, *51*, 204.
(29) Gray, H. B.; Winkler, J. R. *Proc. Natl. Acad. Sci. U.S.A.* **2005**, *102*, 3534.
(30) Hopfield, J. J. *Proc. Natl Acad. Sci. U.S.A.* **1974**, *71*, 3640.
(31) Mayo, S. L.; Ellis, W. R. J.; Crutchley, R. J.; Gray, H. B. *Science* **1986**, *233*, 948.
(32) Moser, C. C.; Keske, J. M.; Warncke, K.; Farid, R. S.; Dutton, P. L. *Nature* **1992**, *355*, 796.
(33) Page, C. C.; Moser, C. C.; Chen, X.; Dutton, P. L. *Nature* **1999**, *402*, 47.
(34) Jortner, J. *J. Chem. Phys.* **1976**, *64*, 4860.
(35) Page, C. C.; Moser, C. C.; Dutton, P. L. *Curr. Opin. Chem. Biol.* **2003**, *7*, 551.
(36) Beratan, D. N.; Onuchic, J. N.; Winkler, J. R.; Gray, H. B. *Science* **1992**, *258*, 1740.
(37) Winkler, J. R.; Gray, H. B. *Chem. Rev.* **1992**, *92*, 369.
(38) Pilet, E.; Jasaitis, A.; Liebl, U.; Vos, M. H. *Proc. Natl Acad. Sci. U.S.A.* **2004**, *101*, 16198.
(39) Jasaitis, A.; Rappaport, F.; Pilet, E.; Liebl, U.; Vos, M. H. *Proc. Natl. Acad. Sci. U.S.A.* **2005**, *102*, 10882.
(40) Moser, C. C.; Page, C. C.; Dutton, P. L. *Philos. Trans. R. Soc. London, B: Biol. Sci.* **2006**, *361*, 1295.
(41) Jasaitis, A.; Johansson, M. P.; Wikström, M.; Vos, M. H.; Verkhovsky, M. I. *Proc. Natl. Acad. Sci. U.S.A.* **2007**, *104*, 20811.
(42) Beratan, D. N.; Balabin, I. A. *Proc. Natl. Acad. Sci U.S.A.* **2008**, *105*, 403.
(43) Marcus, R. A. *J. Phys. Chem.* **1968**, *72*, 891.
(44) Silverman, D. N.; Tu, C.; Chen, X.; Tanhauser, S. M.; Kresge, A. J.; Laipis, P. J. *Biochemistry* **1993**, *32*, 10757.
(45) Silverman, D. N. *Biochim. Biophys. Acta* **2000**, *1458*, 88.
(46) Warshel, A.; Weiss, R. M. *J. Am. Chem. Soc.* **1980**, *102*, 6218.
(47) Schmitt, U. W.; Voth, G. A. *J. Phys. Chem. B* **1998**, *102*, 5547.
(48) Olsson, M. H. M.; Warshel, A. *Proc. Natl. Acad. Sci. U.S.A.* **2006**, *103*, 6500.
(49) Pisliakov, A. V.; Sharma, P. K.; Chu, Z. T.; Haranczyk, M.; Warshel, A. *Proc. Natl. Acad. Sci. U.S.A.* **2008**, *105*, 7726.
(50) Xu, J.; Voth, G. A. *Proc. Natl. Acad. Sci. U.S.A.* **2005**, *102*, 6795.
(51) Xu, J.; Voth, G. A. *Biochim. Biophys. Acta* **2006**, *1757*, 852.
(52) Xu, J.; Sharpe, M. A.; Qin, L.; Ferguson-Miller, S.; Voth, G. A. *J. Am. Chem. Soc.* **2007**, *129*, 2910.
(53) Xu, J.; Voth, G. A. *Biochim. Biophys. Acta* **2008**, *1777*, 196.
(54) Pomès, R.; Roux, B. *Biophys. J.* **1998**, *75*, 33.
(55) Chakrabarti, N.; Tajkhorshid, E.; Roux, B.; Pomès, R. *Structure* **2004**, *12*, 65.
(56) Cui, Q.; Karplus, M. *J. Am. Chem. Soc.* **2002**, *124*, 3093.

(57) Rosta, E.; Woodcock, H. L.; Brooks, B. R.; Hummer, G. *J. Comput. Chem.* **2009**, *30*, 1634.
(58) Dieterich, J. M.; Werner, H. J.; Mata, R. A.; Metz, S.; Thiel, W. *J. Chem. Phys.* **2010**, *132*, 035101.
(59) Warshel, A. *Biochemistry* **1981**, *20*, 3167.
(60) Bashford, D.; Karplus, M. *Biochemistry* **1990**, *29*, 10219.
(61) Koehl, P. *Curr. Opin. Struct. Biol.* **2006**, *16*, 142.
(62) Rabenstein, B.; Knapp, E. W. *Biophys. J.* **2001**, *80*, 1141.
(63) Alexov, E. G.; Gunner, M. R. *Biophys. J.* **1997**, *72*, 2075.
(64) Georgescu, R. E.; Alexov, E. G.; Gunner, M. R. *Biophys. J.* **2002**, *83*, 1731.
(65) Kannt, A.; Lancaster, C. R.; Michel, H. *Biophys. J.* **1998**, *74*, 708.
(66) Popovic, D. M.; Stuchebrukhov, A. A. *FEBS Lett.* **2004**, *566*, 126.
(67) Popovic, D. M.; Quenneville, J.; Stuchebrukhov, A. A. *J. Phys. Chem. B* **2005**, *109*, 3616.
(68) Makhov, D. V.; Popovic, D. M.; Stuchebrukhov, A. A. *J. Phys. Chem. B* **2006**, *110*, 12162.
(69) Song, Y.; Michonova-Alexova, E.; Gunner, M. R. *Biochemistry* **2006**, *45*, 7959.
(70) Fadda, E.; Chakrabarti, N.; Pomès, R. *J. Phys. Chem. B* **2005**, *109*, 22629.
(71) Fadda, E.; Yu, C. H.; Pomès, R. *Biochim. Biophys. Acta* **2008**, *1777*, 277.
(72) Tuukkanen, A.; Verkhovsky, M. I.; Laakkonen, L.; Wikström, M. *Biochim. Biophys. Acta* **2006**, *1757*, 1117.
(73) Olkhova, E.; Helms, V.; Michel, H. *Biophys. J.* **2005**, *89*, 2324.
(74) Ghosh, N.; Xavier, P.-R.; Gunner, M. R.; Cui, Q. *Biochemistry* **2009**, *48*, 2468.
(75) Borgis, D.; Hynes, J. T. *Chem. Phys.* **1993**, *170*, 315.
(76) Borgis, D.; Hynes, J. T. *J. Chem. Phys.* **1991**, *94*, 3619.
(77) Hwang, J.-K.; Chu, Z. T.; Yadav, A.; Warshel, A. *J. Phys. Chem.* **1991**, *95*, 8445.
(78) Marx, D.; Tuckerman, M. E.; Hutter, J.; Parrinello, M. *Nature* **1999**, *379*, 601.
(79) Pomès, R.; Roux, B. *Biophys. J.* **1996**, *71*, 19.
(80) Villa, J.; Warshel, A. *J. Phys. Chem. B* **2001**, *105*, 7887.
(81) Cukier, R. I.; Nocera, D. G. *Annu. Rev. Phys. Chem.* **1998**, *49*, 337.
(82) Hammes-Schiffer, S. *Acc. Chem. Res.* **2001**, *34*, 273.
(83) Hammes-Schiffer, S.; Soudackov, A. V. *J. Phys. Chem. B* **2008**, *112*, 14108.
(84) Graige, M. S.; Paddock, M. L.; Bruce, J. M.; Feher, G.; Okamura, M. Y. *J. Am. Chem. Soc.* **1996**, *118*, 9005.
(85) Faller, P.; Goussias, C.; Rutherford, A. W.; Un, S. *Proc. Natl. Acad. Sci. U.S.A.* **2003**, *100*, 8732.
(86) Nagle, J. F.; Morowitz, H. J. *Proc. Natl. Acad. Sci. U.S.A.* **1978**, *75*, 298.
(87) Agmon, A. *Chem. Phys. Lett.* **1995**, *244*, 456.
(88) Wraight, C. A. *Biochim. Biophys. Acta* **2006**, *1757*, 886.
(89) Ahlrichs, R.; Bär, M.; Häser, M.; Horn, H.; Kölmel, C. *Chem. Phys. Lett.* **1989**, *162*, 165.
(90) Hassan, S. A.; Hummer, G.; Lee, Y.-S. *J. Chem. Phys.* **2006**, *124*, 204510-1–8.
(91) Dellago, C.; Naor, M. M.; Hummer, G. *Phys. Rev. Lett.* **2003**, *90*, 105902-1–4.
(92) Dellago, C.; Hummer, G. *Phys. Rev. Lett.* **2006**, *97*, 245901-1–4.
(93) Lapid, H.; Agmon, N.; Petersen, M. K.; Voth, G. A. J. *Chem. Phys.* **2005**, *122*, 14506-1–11.
(94) Markovitch, O.; Chen, H.; Izvekov, S.; Paesani, F.; Voth, G.; Agmon, N. *J. Phys. Chem. B* **2008**, *112*, 9456.
(95) Lee, Y. S.; Krauss, M. *J. Am. Chem. Soc.* **2004**, *126*, 2225.
(96) Lehle, H.; Krieg, J. M.; Nienhaus, K.; Deng, P.; Fengler, S.; Nienhaus, G. U. 2005, *88*, 1978.
(97) Vaitheeswaran, S.; Rasaiah, J. C.; Hummer, G. *J. Chem. Phys.* **2004**, *121*, 7955.
(98) Rasaiah, J. C.; Garde, S.; Hummer, G. *Annu. Rev. Phys. Chem.* **2008**, *59*, 713.
(99) Tieleman, D. P. *BMC Biochem.* **2004**, *5*, 10–1.
(100) Wraight, C. A. *Front. Biosci.* **2004**, *9*, 309.
(101) Antalis, T. M.; Palmer, G. *J. Biol. Chem.* **1982**, *257*, 6194.
(102) Rieder, R.; Bosshard, H. R. *J. Biol. Chem.* **1980**, *255*, 4732.
(103) Witt, H.; Zickermann, V.; Ludwig, B. *Biochim. Biophys. Acta* **1995**, *1230*, 74.
(104) Millet, F.; de Jong, C.; Paulson, L.; Capaldi, R. *Biochemistry* **1983**, *22*, 546.
(105) Kroneck, P. M.; Antholine, W. E.; Kastrau, D. H.; Buse, G.; Steffens, G. C.; Zumft, W. G. *FEBS Lett.* **1990**, *268*, 274.
(106) Wikström, M.; Krab, K.; Saraste, M. *Cytochrome oxidase—A synthesis*; Academic Press: London and New York, 1981.
(107) Johansson, M. P.; Kaila, V. R. I.; Laakkonen, L. *J. Comput. Chem.* **2007**, *29*, 753.
(108) Karpefors, M.; Slutter, C. E.; Fee, J. A.; Aasa, R.; Kallebring, B.; Larsson, S.; Vanngard, T. *Biophys. J.* **1996**, *71*, 2823.
(109) Bertini, I.; Bren, K. L.; Clemente, A.; Fee, J. A.; Gray, H. B.; Luchinat, C.; Malmström, B. G.; Richards, J. H.; Sanders, D.; Slutter, C. E. *J. Am. Chem. Soc.* **1996**, *118*, 11658.
(110) Northrup, S. H.; Erickson, H. P. *Proc. Natl. Acad. Sci. U.S.A.* **1992**, *89*, 3338.
(111) Geren, L. M.; Beasley, J. R.; Fine, B. R.; Saunders, A. J.; Hibdon, S.; Pielak, G. J.; Durham, B.; Millett, F. *J. Biol. Chem.* **1995**, *270*, 2466.
(112) Hill, B. C. *J. Biol. Chem.* **1991**, *266*, 2219.
(113) Hill, B. C. *J. Biol. Chem.* **1994**, *269*, 2419.
(114) Roberts, V. A.; Pique, M. E. *J. Biol. Chem.* **1999**, *274*, 38051.
(115) Johansson, M. P.; Blomberg, M. R. A.; Sundholm, D.; Wikström, M. *Biochim. Biophys. Acta* **2002**, *1553*, 183.
(116) Johansson, M. P.; Sundholm, D.; Gerfen, G.; Wikström, M. *J. Am. Chem. Soc.* **2002**, *124*, 11771.
(117) Ädelroth, P.; Brzezinski, P.; Malmström, B. G. *Biochemistry* **1995**, *34*, 2844.
(118) Ruitenberg, M.; Kannt, A.; Bamberg, E.; Ludwig, B.; Michel, H.; Fendler, K. *Proc. Natl. Acad. Sci. U.S.A.* **2000**, *97*, 4632.
(119) Belevich, I.; Bloch, D. A.; Belevich, N.; Wikström, M.; Verkhovsky, M. I. *Proc. Natl. Acad. Sci. U.S.A.* **2007**, *104*, 2685.
(120) Bloch, D.; Belevich, I.; Jasaitis, A.; Ribacka, C.; Puustinen, A.; Verkhovsky, M. I.; Wikström, M. *Proc. Natl. Acad. Sci. U.S.A.* **2004**, *101*, 529.
(121) Morgan, J. E.; Li, P. M.; Jang, D. J.; El Sayed, M. A.; Chan, S. I. *Biochemistry* **1989**, *28*, 6975.
(122) Oliveberg, M.; Malmström, B. G. *Biochemistry* **1991**, *30*, 7053.
(123) Verkhovsky, M. I.; Morgan, J. E.; Wikström, M. *Biochemistry* **1992**, *31*, 11860.
(124) Oliveberg, M.; Brzezinski, P.; Malmström, B. G. *Biochim. Biophys. Acta* **1989**, *977*, 322.
(125) Siletsky, S. A.; Pawate, A. S.; Weiss, K.; Gennis, R. B.; Konstantinov, A. A. *J. Biol. Chem.* **2004**, *279*, 52558.
(126) Woodruff, W. H.; Einarsdóttir, O.; Dyer, R. B.; Bagley, K. A.; Palmer, G.; Atherton, S. J.; Goldbeck, R. A.; Dawes, T. D.; Kliger, D. S. *Proc. Natl. Acad. Sci. U.S.A.* **1991**, *88*, 2588.
(127) Morgan, J. E.; Verkhovsky, M. I.; Puustinen, A.; Wikström, M. *Biochemistry* **1993**, *32*, 11413.
(128) Verkhovsky, M. I.; Jasaitis, A.; Wikström, M. *Biochim. Biophys. Acta* **2001**, *1506*, 143.
(129) Brändén, M.; Namslauer, A.; Hansson, O.; Aasa, R.; Brzezinski, P. *Biochemistry* **2003**, *42*, 13178.
(130) Belevich, I.; Tuukkanen, A.; Wikström, M.; Verkhovsky, M. I. *Biochemistry* **2006**, *45*, 4000.
(131) Power, G. G.; Stegall, H. *J. Appl. Physiol.* **1970**, *29*, 145.
(132) Tsukihara, T.; Aoyama, H.; Yamashita, E.; Tomizaki, T.; Yamaguchi, H.; Shinzawa-Itoh, K.; Nakashima, R.; Yaono, R. S. Y. *Science* **1996**, *272*, 1136.
(133) Iwata, S.; Ostermeier, C.; Ludwig, B.; Michel, H. *Nature* **1995**, *376*, 660.
(134) Ostermeier, C.; Harrenga, A.; Ermler, U.; Michel, H. *Proc. Natl. Acad. Sci. U.S.A.* **1997**, 10547.
(135) Svensson-Ek, M.; Abramson, J.; Larsson, G.; Tornroth, S.; Brezezinski, P.; Iwata, S. *J. Mol. Biol.* **2002**, *321*, 329.
(136) Soulimane, T.; Buse, G.; Bourenkov, G. P.; Bartunik, H. D.; Huber, R.; Than, M. E. *EMBO J.* **2000**, *19*, 1766.
(137) Abramson, J.; Riistama, S.; Larsson, G.; Jasaitis, A.; Svensson-Ek, M.; Laakkonen, L.; Puustinen, A.; Iwata, S.; Wikström, M. *Nat. Struct. Biol.* **2000**, *7*, 910.
(138) Qin, L.; Hiser, C.; Mulichak, A.; Garavito, R. M.; Ferguson-Miller, S. *Proc. Natl. Acad. Sci. U.S.A.* **2006**, *103*, 6117.
(139) Koepke, J.; Olkhova, E.; Angerer, H.; Muller, H.; Peng, G.; Michel, H. *Biochim. Biophys. Acta* **2009**, *1787*, 635.
(140) Aoyama, H.; Muramoto, K.; Shinzawa-Itoh, K.; Hirata, K.; Yamashita, E.; Tsukihara, T.; Ogura, T.; Yoshikawa, S. *Proc. Natl. Acad. Sci. U.S.A.* **2009**, *106*, 2165.
(141) Qin, L.; Liu, J.; Mills, D.; Proshlyakov, D. A.; Hiser, C.; Ferguson-Miller, S. *Biochemistry* **2009**, *48*, 5121.
(142) Riistama, S.; Puustinen, A.; Garcia-Horsman, A.; Iwata, S.; Michel, H.; Wikström, M. *Biochim. Biophys. Acta* **1996**, *1275*, 1.
(143) Hofacker, I.; Schulten, K. *Proteins* **1998**, *86*, 100.
(144) Chance, B.; Saronio, C.; Leigh, J. S. *J. Biol. Chem.* **1975**, *250*, 9226.
(145) Hill, B. C.; Greenwood, C. *Biochem. J.* **1983**, *215*, 659.
(146) Verkhovsky, M. I.; Morgan, J. E.; Wikström, M. *Biochemistry* **1994**, *33*, 3079.
(147) Verkhovsky, M. I.; Morgan, J. E.; Puustinen, A.; Wikström, M. *Nature* **1996**, *380*, 268.
(148) Petersen, L. C.; Nicholls, P.; Degn, H. *Biochem. J.* **1974**, *142*, 247.
(149) Wikström, M. *Proc. Natl. Acad. Sci. U.S.A.* **1981**, *78*, 4051.
(150) Weng, L. C.; Baker, G. M. *Biochemistry* **1991**, *30*, 5727.
(151) Morgan, J. E.; Verkhovsky, M. I.; Wikström, M. *Biochemistry* **1996**, *35*, 12235.

(152) Proshlyakov, D. A.; Ogura, T.; Shinzawa-Itoh, K.; Yoshikawa, S.; Appelman, E. H.; Kitagawa, T. *J. Biol. Chem.* **1994**, *269*, 29385.
(153) Proshlyakov, D. A.; Ogura, T.; Shinzawa-Itoh, K.; Yoshikawa, S.; Kitagawa, T. *Biochemistry* **1996**, *35*, 76.
(154) Proshlyakov, D. A.; Pressler, M. A.; Babcock, G. T. *Proc. Natl. Acad. Sci. U.S.A.* **1998**, *95*, 8020.
(155) Fabian, M.; Wong, W. W.; Gennis, R. B.; Palmer, G. *Proc. Natl. Acad. Sci. U.S.A.* **1999**, *96*, 12971.
(156) Ferguson-Miller, S.; Babcock, G. T. *Chem. Rev.* **1996**, *96*, 2889.
(157) Morgan, J. E.; Verkhovsky, M. I.; Palmer, G.; Wikström, M. *Biochemistry* **2001**, *40*, 6882.
(158) Hansson, Ö.; Karlsson, B.; Aasa, R.; Vänngård, T.; Malmström, B. G. *EMBO J.* **1982**, *1*, 1295.
(159) Laaksonen, L. J. *Mol. Graphics* **1992**, *10*, 33.
(160) Bergman, D. L.; Laaksonen, L.; Laaksonen, A. J. *Mol. Graph. Model.* **1997**, *15*, 301.
(161) Gorbikova, E. A.; Belevich, I.; Wikström, M.; Verkhovsky, M. I. *Proc. Natl. Acad. Sci. U.S.A.* **2008**, *105*, 10733.
(162) Babcock, G. T. *Proc. Natl Acad. Sci. U.S.A.* **1999**, *96*, 12971.
(163) Proshlyakov, D. A.; Pressler, M. A.; DeMaso, C.; Leykam, J. F.; DeWitt, D. L.; Babcock, G. T. *Science* **2000**, *290*, 1588.
(164) Blomberg, M. R. A.; Siegbahn, P. E. M.; Wikström, M. *Inorg. Chem.* **2003**, *42*, 5231.
(165) Blomberg, M. R. A.; Siegbahn, P. E. M.; Babcock, G. T.; Wikström, M. *J. Am. Chem. Soc.* **2000**, *122*, 12848.
(166) Blomberg, M. R. A.; Siegbahn, P. E. M. *Biochim. Biophys. Acta* **2010**, *1797*, 129.
(167) Brändèn, M.; Sigurdson, H.; Namslauer, A.; Gennis, R. B.; Ädelroth, P.; Brzezinski, P. *Proc. Natl. Acad. Sci. U.S.A.* **2001**, *98*, 5013.
(168) Lepp, H.; Svahn, E.; Faxen, K.; Brzezinski, P. *Biochemistry* **2008**, *47*, 4929.
(169) Wikström, M.; Verkhovsky, M. I. *Biochim. Biophys. Acta* **2006**, *1757*, 1047.
(170) Goodin, D. B.; McRee, D. E. *Biochemistry* **1993**, *32*, 3313.
(171) Rich, P. R.; Iwaki, M. *Biochemistry (Moscow)* **2007**, *72*, 1047.
(172) Hersleth, H. P.; Ryde, U.; Rydberg, P.; Görbitz, C. H.; Andersson, K. K. *J. Inorg. Biochem.* **2006**, *100*, 460.
(173) Gorbikova, E. A.; Wikström, M.; Verkhovsky, M. I. *J. Biol. Chem.* **2008**, *283*, 34907.
(174) Siletsky, S. A.; Belevich, I.; Jasaitis, A.; Konstantinov, A. A.; Wikström, M.; Soulimane, T.; Verkhovsky, M. I. *Biochim. Biophys. Acta* **2007**, *1767*, 1383.
(175) Verkhovsky, M. I.; Jasaitis, A.; Verkhovskaya, M. L.; Morgan, J. E.; Wikström, M. *Nature* **1999**, *400*, 480.
(176) Wiertz, F. G.; Richter, O. M.; Cherepanov, A. V.; MacMillan, F.; Ludwig, B.; de Vries, S. *FEBS Lett.* **2004**, *575*, 127.
(177) Wiertz, F. G.; Richter, O. M.; Ludwig, B.; de Vries, S. *J. Biol. Chem.* **2007**, *282*, 31580.
(178) Han, S.; Ching, Y. C.; Rousseau, D. L. *Nature* **1990**, *348*, 89.
(179) Han, S.; Takahashi, S.; Rousseau, D. L. *J. Biol. Chem.* **2000**, *275*, 1910.
(180) Wilson, M. T.; Peterson, J.; Antonini, E.; Brunori, M.; Colosimo, A.; Wyman, J. *Proc. Natl. Acad. Sci. U.S.A.* **1981**, *78*, 7115.
(181) Moody, A. J.; Cooper, C. E.; Rich, P. R. *Biochim. Biophys. Acta* **1991**, *1059*, 189.
(182) Brunori, M.; Giuffre, A.; Sarti, P. *J. Inorg. Biochem.* **2005**, *99*, 324.
(183) Jancura, D.; Berka, V.; Antalik, M.; Bagelova, J.; Gennis, R. B.; Palmer, G.; Fabian, M. *J. Biol. Chem.* **2006**, *281*, 30319.
(184) Gorbikova, E. A.; Vuorilehto, K.; Wikström, M.; Verkhovsky, M. I. *Biochemistry* **2006**, *45*, 5641.
(185) Kim, E.; Chufán, E. E.; Kamaraj, K.; Karlin, K. D. *Chem. Rev.* **2004**, *104*, 1077.
(186) Henry, R. M.; Yu, C. H.; Rodinger, T.; Pomès, R. *J. Mol. Biol.* **2009**, *387*, 1165.
(187) Riistama, S.; Hummer, G.; Puustinen, A.; Dyer, R. B.; Woodruff, W. H.; Wikström, M. *FEBS Lett.* **1997**, *414*, 275.
(188) Zheng, X.; Medvedev, D. M.; Swanson, J.; Stuchebrukhov, A. A. *Biochim. Biophys. Acta* **2003**, *1557*, 99.
(189) Tuukkanen, A.; Kaila, V. R. I.; Laakkonen, L.; Hummer, G.; Wikström, M. *Biochim. Biophys. Acta* **2007**, *1767*, 1102.
(190) Wikström, M.; Verkhovsky, M. I.; Hummer, G. *Biochim. Biophys. Acta* **2003**, *1604*, 61.
(191) Seibold, S. A.; Mills, D. A.; Ferguson-Miller, S.; Cukier, R. I. *Biochemistry* **2005**, *44*, 10475–10485.
(192) Pawate, A. S.; Morgan, J.; Namslauer, A.; Mills, D.; Brzezinski, P.; Ferguson-Miller, S.; Gennis, R. B. *Biochemistry* **2002**, *41*, 13417.
(193) Namslauer, A.; Pawate, A. S.; Gennis, R. B.; Brzezinski, P. *Proc. Natl. Acad. Sci. U.S.A.* **2003**, *100*, 15543.
(194) Dürr, K. L.; Koepke, J.; Hellwig, P.; Müller, H.; Angerer, H.; Peng, G.; Olkhova, E.; Richter, O. M.; Ludwig, B.; Michel, H. *J. Mol. Biol.* **2008**, *384*, 865.
(195) Kaila, V. R. I.; Verkhovsky, M. I.; Hummer, G.; Wikström, M. *Biochim. Biophys. Acta* **2009**, *1787*, 1205.
(196) Kaila, V. R. I.; Verkhovsky, M. I.; Hummer, G.; Wikström, M. *Proc. Natl. Acad. Sci* **2008**, *105*, 6255.
(197) Vygodina, T. V.; Pecoraro, C.; Mitchell, D.; Gennis, R.; Konstantinov, A. A. *Biochemistry* **1998**, *37*, 3053.
(198) Ädelroth, P.; Gennis, R. B.; Brzezinski, P. *Biochemistry* **1998**, *37*, 2470.
(199) Wikström, M.; Jasaitis, A.; Backgren, C.; Puustinen, A.; Verkhovsky, M. I. *Biochim. Biophys. Acta* **2000**, *1459*, 514.
(200) Morgan, J. E.; Verkhovsky, M. I.; Wikström, M. *J. Bioenerg. Biomembr.* **1994**, *26*, 599.
(201) Rich, P. R.; Austr, J. *Plant Physiol.* **1995**, *22*, 479.
(202) Michel, H. *Biochemistry* **1999**, *38*, 15129.
(203) Belevich, I.; Verkhovsky, M. I.; Wikström, M. *Nature* **2006**, *440*, 829.
(204) Siegbahn, P. E. M.; Blomberg, M. R. A. *Biochim. Biophys. Acta* **2007**, *1767*, 1143.
(205) Kaila, V. R. I.; Sharma, V.; Wikström, M. *Biochim. Biophys. Acta*, in press.
(206) Kim, Y. C.; Wikström, M.; Hummer, G. *Proc. Natl. Acad. Sci. U.S.A.* **2007**, *104*, 2169.
(207) Kim, Y. C.; Wikström, M.; Hummer, G. *Proc. Natl. Acad. Sci. U.S.A.* **2009**, *106*, 13707.
(208) Ädelroth, P.; Ek, M. S.; Mitchell, D. M.; Gennis, R. B.; Brzezinski, P. *Biochemistry* **1997**, *36*, 13824.
(209) Blomberg, M. R. A.; Siegbahn, P. E. M. *Biochim. Biophys. Acta* **2010**, *1797*, 129.
(210) Brzezinski, P.; Larsson, G. *Biochim. Biophys. Acta* **2003**, *1605*, 1.
(211) Salomonsson, L.; Faxen, K.; Ädelroth, P.; Brzezinski, P. *Proc. Natl. Acad. Sci. U.S.A.* **2005**, *102*, 17624.
(212) Jasaitis, A.; Backgren, C.; Morgan, J. E.; Puustinen, A.; Verkhovsky, M. I.; Wikström, M. *Biochemistry* **2001**, *40*, 5269.
(213) Faxén, K.; Gilderson, G.; Ädelroth, P.; Brzezinski, P. *Nature* **2005**, *437*, 286.
(214) Rich, P. R.; Meunier, B.; Mitchell, R.; Moody, A. J. *Biochim. Biophys. Acta* **1996**, *1275*, 91.
(215) Tommos, C.; Babcock, G. T. *Biochim. Biophys. Acta* **2000**, *1458*, 199.
(216) Pratt, D. A.; Pesavento, R. P.; van der Donk, W. A. *Org. Lett.* **2005**, *7*, 2735.
(217) Moore, G. R.; Pettigrew, G. W. *Cytochromes c, Evolutionary, Structural and Physicochemical Aspects*; Springer Verlag: Berlin, 1990.
(218) Siegbahn, P. E. M.; Blomberg, M. R. A. *J. Phys. Chem. A* **2008**, *112*, 12772.
(219) Mitchell, R.; Rich, P. R. *Biochim. Biophys. Acta* **1994**, *1186*, 19.
(220) Verkhovsky, M. I.; Belevich, N.; Morgan, J. E.; Wikström, M. *Biochim. Biophys. Acta* **1999**, *1412*, 184.
(221) Forte, E.; Barone, M. C.; Brunori, M.; Sarti, P.; Giuffre, A. *Biochemistry* **2002**, *41*, 13046.
(222) Parul, D.; Palmer, G.; Fabian, M. *Biochemistry* **2005**, *44*, 4562.
(223) Oliveberg, M.; Hallen, S.; Nilsson, T. *Biochemistry* **1991**, *30*, 436.
(224) Popovic, D. M.; Stuchebrukhov, A. A. *J. Am. Chem. Soc.* **2004**, *126*, 1858.
(225) Wikström, M.; Ribacka, C.; Molin, M.; Laakkonen, L.; Verkhovsky, M.; Puustinen, A. *Proc. Natl. Acad. Sci. U.S.A.* **2005**, *102*, 10478.
(226) Leontyev, I. V.; Stuchebrukhov, A. A. *J. Vhem. Theory Comput.* **2010**, *6*, 1498.
(227) Phillips, J. C.; Braun, R.; Wang, W.; Gumbart, J.; Tajkhorshid, E.; Villa, E.; Chipot, C.; Skeel, R. D.; Kale, L.; Schulten, K. *J. Comput. Chem.* **2005**, *26*, 1781.
(228) MacKerell, A. D.; et al. *J. Phys. Chem. B* **1998**, *102*, 3586.
(229) Lanyi, J. K. *Biochim. Biophys. Acta* **2005**, *1757*, 1012.

CR1002003